Ecological Informatics 95 (2026) 103716

Contents lists available at ScienceDirect

Ecological Informatics

journal homepage: www.elsevier.com/locate/ecolinf

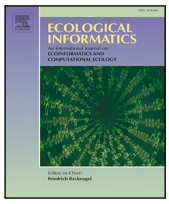

A new framework for measuring community diversity in temporal ecological networks

Zakariya Ghalmane [a,b,*], Pascal Poncelet [b], Roberto Interdonado [c,e], Dino Ienco [d,e], Pierluigi Carbonara [f], Angelo Cau [g], Antonio Esteban [h], Maria Teresa Farriols [i], Maria Cristina Follesa [g], Cristina Garcia-Ruiz [j], Germana Garofalo [k], Gioacchino Bono [k], Taha Imzilen [l], Igor Isajlović [m], Stefanos Kavadas [n], Irida Maina [n], Porzia Maiorano [o], Chiara Manfredi [p], Jurgen Mifsud [q], Panagiota Peristeraki [r], Mario Sbrana [s], Maria Teresa Spedicato [f], Ioannis Thasitis [t], Nedo Vrgoc [m], Bastien Mérigot [l]

[a] CESI LINEACT, UR 7527, Strasbourg, France
[b] LIRMM, University of Montpellier, Montpellier, France
[c] CIRAD, TETIS, Montpellier, France
[d] INRAE, TETIS, Montpellier, France
[e] EVERGREEN, University of Montpellier, Inria, Montpellier, France
[f] COISPA Tecnologia e Ricerca, Bari, Italy
[g] Department of Life and Environmental Science, University of Cagliari, Cagliari, Italy
[h] Instituto Español de Oceanografía (IEO), Centro Oceanográfico de Murcia, Murcia, Spain
[i] Instituto Español de Oceanografía (IEO), Centre Oceanogràfic de les Balears, Palma, Spain
[j] Instituto Español de Oceanografía (IEO-CSIC), Centro Oceanográfico de Málaga, Málaga, Spain
[k] Institute for Biological Resources and Marine Biotechnology, National Research Council (CNR-IRBIM), Mazara del Vallo, Italy
[l] MARBEC, Univ Montpellier, IRD, IFREMER, CNRS, Sète, France
[m] Institute of Oceanography and Fisheries, Split, Croatia
[n] Institute of Marine Biological Resources and Inland Waters, Hellenic Centre for Marine Research, Anavyssos, Greece
[o] Department of Bioscience, Biotechnology and Environment, University of Bari Aldo Moro, Bari, Italy
[p] Laboratorio di Biologia Marina e Pesca, Dip.to BiGeA, Università di Bologna, Fano, Italy
[q] Department of Fisheries and Aquaculture, Ministry for Agriculture, Fisheries, Food and Animal Rights, Marsa, Malta
[r] Institute of Marine Biological Resources and Inland Waters, Hellenic Centre for Marine Research, Heraklion, Crete, 71003, Greece
[s] Consorzio per il Centro Interuniversitario di Biologia Marina ed Ecologia Applicata, Livorno, Italy
[t] Department of Fisheries and Marine Research, Ministry of Agriculture, Natural Resources and Environment, Nicosia, Cyprus

ARTICLE INFO

Dataset link: https://github.com/zakariyaGH/METITS_and_bats_Studies, https://doi.org/10.3989/scimar.2019.83S1, https://data.jrc.ec.europa.eu/dataset/f25092c4-3f0f-449f-ba60-5fbfe385defc, https://idata.idiv.de/ddm/Data/ShowData/286

Keywords:
Diversity
Function
Phylogeny
Taxonomy
Complex networks
Centrality measure

ABSTRACT

Assessing changes in community diversity is a central issue with regard to many fundamental and applied aspects in ecology, biogeography and conservation. However, some important features for the assessment of community by diversity measures still need to be considered to quantify spatio-temporal variation, notably their explicit variation through time while integrating network structure and species differences. Here we introduce a new framework based on complex network analysis and on an extension of Hill numbers. It encompasses three main aspects: i) the differences/distances between species (e.g., co-occurrence, function, phylogeny, taxonomy), ii) the topological properties of the network, and iii) the variability along the time dimension by introducing three measures quantifying the overall temporal dynamics of the network. To illustrate how the new framework reveals complementary patterns beyond those identified by traditional approaches in previous studies, we analyze two data sets that vary in both their temporal extent and the types of communities they represent: (i) Mediterranean exploited fish communities sampled during 25 years, (ii) Amazonian bat communities surveyed during 4 years. Our results showed that the fish communities could be classified into five different clusters according to their spatio-temporal behaviors, as well as environmental and fishing forcings. Bat community diversity has higher values in larger forest fragment areas, while habitats with small areas exhibit very high

* Corresponding author.
E-mail address: zghalmane@cesi.fr (Z. Ghalmane).

https://doi.org/10.1016/j.ecoinf.2026.103716
Received 3 November 2023; Received in revised form 10 March 2026; Accepted 13 March 2026
Available online 2 April 2026

changes through time mainly due to species turnover. By simultaneously incorporating essential features of communities, the new framework enhances identification of their spatio-temporal trends, and helps to identify priority zones of interest for management and conservation.

1. Introduction

Developing advanced methods able to describe the spatial and temporal variation of community diversity is one of the most critical challenges in the current context of assessing and predicting biodiversity trajectories and their underlying processes, notably in response to global change (Sutherland et al., 2013; Socolar et al., 2016; Magurran and McGill, 2011; Magurran, 2013). Community diversity is widely quantified using measures based on species presence-absence or proportions (e.g., derived from abundance, biomass or coverage), as well as species differences (i.e., taxonomy, phylogeny or function). A plethora of diversity indices and frameworks have been designed to analyze community diversity (Loiseau et al., 2017; Chao and Chiu, 2016; Chao et al., 2014; Delmas et al., 2019; Siwicka et al., 2020). Numerous diversity indices are available to evaluate the different facets of community diversity. For instance, species richness (S), which measures the number of species in a sample, is still one of the most widely used measures. Other indices, such as the Simpson and Shannon diversity indices, quantify in a single value both species richness and evenness (i.e., the distribution of individuals among species) with varying sensitivities to dominant or rare species, respectively (Peet, 1974). Based on these indices, the Simpson and Pielou evenness indices focus specifically on the evenness component (Smith and Wilson, 1996). In addition, complementary indices take into account species differences, such as taxonomic, phylogenetic, or functional differences. The latter are computed using various distance or dissimilarity indices based on a species-attribute matrix. Functional distances denote differences in ecological attributes or roles among species (e.g., feeding habits, resource utilization, or physiological features (Violle et al., 2007)). Taxonomic distances, in contrast, refer to the hierarchical classification of species based on shared morphological features, while phylogenetic distances represent the evolutionary relationships between species often assessed through molecular differences. One index that accounts for these species differences is Rao's quadratic entropy, among others. This index extends the Simpson diversity index by considering species distances and is defined as the mean distance between two randomly selected individuals (or species, for presence-absence data) within a community (Rao, 1982; Pavoine, 2012). These indices have been used extensively for both terrestrial and marine ecosystems (Devictor et al., 2010; Lefcheck et al., 2014; Mouillot et al., 2011; Stuart-Smith et al., 2013; Granger et al., 2015). In addition, several existing approaches quantify temporal community dynamics from species by time matrices, for example through summary measures of compositional change and stability, or through temporal beta diversity decomposition. The R packages codyn and betapart (Hallett et al., 2016; Baselga and Orme, 2012) provide widely used toolkits for such analyses, including turnover and nestedness components and a suite of community dynamics measures. However, these approaches do not explicitly integrate network structure and species difference layers into a unified temporal diversity framework, for enabling the detection of temporal change in both composition and co-occurrence structure.

In contrast to these indices, Hill numbers provide a framework to characterize the diversity of an assemblage through a unified formula. They were first developed by Hill (1973), and later reintroduced to ecology by Jost (2006, 2007). Hill numbers are defined based on the parameter q which determines sensitivity to the relative proportions of species. The Hill numbers represent the effective number of species (i.e. true diversity) and, depending on the q value, they mathematically correspond to species richness (q = 0), the exponential of Shannon's entropy (q = 1), or the inverse of the Simpson (q = 2). A more detailed description of Hill numbers is provided in the next section. Building on Hill numbers and a proportion component, a framework was recently proposed by Ohlmann et al. (2019) to enhance diversity assessments. Initially, the proportion was computed based on species abundance. Subsequently, it was also computed based on the frequency of "associations" between species (e.g., co-occurrence) and the abundance of links (a combination of species abundance and their co-occurrence). This proposed framework measures diversity at three scales: locally (α-diversity), regionally (γ-diversity) and among different spatial or temporal units (β-diversity). Hill numbers are applicable across all three of these diversity scales. Diversity can also be measured in contexts beyond community diversity. For instance, Martínez-López et al. (2023) proposed a measure to assess the habitat diversity within protected areas (PA). The measure, termed "Terrestrial Habitat diversity (THD)", combines two components. The first is the count of terrestrial and marine eco-regions present in or adjacent to the PA under study, while the second is Shannon's diversity index, computed using the proportions derived from the relative abundance of each habitat within a PA. Consequently, a higher THD value indicates greater habitat diversity in terms of eco-regions and equally represented habitats.

Over the past two decades, assemblages of species have increasingly been represented as networks (Tylianakis and Morris, 2017; Ohlmann et al., 2019; Jacoby and Freeman, 2016; Legras et al., 2019a; Interdonato et al., 2017) where nodes represent species and links represent their "associations". An "association" simultaneously captures the co-occurrence of species (derived from presence-absence data, abundance, biomass, coverage, etc.) and their taxonomic, phylogenetic, or functional differences when such data are available. However, it is crucial to consider the network's topology when calculating diversity metrics based on species presence-absence or proportions within an assemblage. The topology of the network refers to the arrangement of nodes (species) and edges (interactions), encompassing the structural patterns and connectivity that define the network's overall architecture. This distinction is important to identify cases where two species assemblages share the same diversity value using one of the existing indices, but possess entirely different topological characteristics. As such, further improvements in existing diversity indices are essential to account for the topology of networks, thereby providing a more comprehensive and precise understanding of community structure and dynamics.

Moreover, the diversity of species assemblages and network topology can change over time. Some species may increase in proportion, while others may appear, decline or even disappear. The diversity of the different timestamps of an assemblage can be assessed by using the framework proposed by Ohlmann et al. (2019). In this approach, the β-diversity is computed to compare assemblages across various timestamps. Nevertheless, greater emphasis could be placed on assessing the overall progression of patterns of change in diversity over time, which would provide a more comprehensive understanding of temporal dynamics. To summarize, traditional diversity indices offer valuable insights by considering components such as species richness, evenness, as well as pairwise differences among species. However, they do not account for and capture the intricate connections and structural patterns within and across ecological communities, which limits our ability to fully grasp the dynamics of community change.

In this context, we aim to propose a new framework that integrates complex network analysis with traditional diversity measures, to offer a more comprehensive and deeper quantification of community diversity by taking into account both (i) the differences among the species (e.g., function, phylogeny, taxonomy), (ii) the topological properties of the network, and (iii) its variability along the time dimension. Incorporating these aspects for the study of community diversity allows for a deeper understanding of the structural organization and inter-relationships among species of assemblages. By investigating the

topology of species networks, researchers can uncover hidden patterns, identify key species and drivers, and elucidate the underlying mechanisms shaping community dynamics. It thus also aims to provide valuable insights for ecosystem management and conservation strategies in the face of global change.

To illustrate how the new framework reveals complementary patterns beyond those identified by traditional approaches in previous studies, we analyze two data sets already investigated that vary in both their temporal extent and the types of communities they represent: (i) Mediterranean exploited fish communities sampled during 25 years, (ii) Amazonian bats communities surveyed during 4 years. The Mediterranean Sea, recognized for its relatively high biodiversity (Coll et al., 2010), is simultaneously one of the most threatened marine regions globally due to environmental changes and intensive fishing (Coll et al., 2012). Traditional studies using static presence-absence maps lacked temporal variability (Lasram et al., 2009; Coll et al., 2012), while investigations employing traditional diversity indices on MED-ITS data (Spedicato et al., 2019) detected no significant temporal patterns, even over extended periods (18 years: 1994–2012 (Granger et al., 2015)). Yet, given complex interactions between environmental and anthropogenic drivers, some features of community diversity may change over time, complementing traditional indices. We also investigate a bat dataset from Central Amazonia (2011–2014 (Farneda et al., 2015)). Their work demonstrated that Amazonian bat responses to fragmentation vary by traits such as body size and diet, with specialists particularly vulnerable to habitat loss. However, the study of variation in bat community diversity over time, which could reveal complementary patterns to those in Farneda et al. (2015), is still lacking. By applying the framework to two ecologically and temporally distinct datasets, we also aim to demonstrate its flexibility and general applicability across systems, beyond a single taxonomic group or ecological setting.

2. Material and methods

This section is organized to introduce the workflow before detailing individual indices. We first describe the stepwise scheme of the framework and the construction of temporal ecological networks, then define strength connectivity and the two overall temporal indices, temporal diversity and temporal variation. Finally, we describe an optional module that computes pairwise community dissimilarity across time units, which can be used when the analysis requires direct time to time comparisons.

2.1. General scheme

The proposed framework consists of successive steps (Fig. 1). First, the network of the studied species assemblage should be constructed to incorporate its structure when assessing diversity. The nodes of the network refer to species and the links (or edges) refer to species co-occurrence. To this end, the co-occurrence matrix is computed using the 1-Bray Curtis index on species proportions (e.g., abundance, biomass, etc.) or the 1-Jaccard index on the presence-absence data (see Section 2.4.1). Additionally, the functional, taxonomic and phylogenetic matrices are defined. Subsequently, the network of species is constructed based on the co-occurrence matrix, with links weighted according to the elements from one of the species difference matrices. Then, the strength connectivity measure is defined. It combines the strength and the centrality of each species. The strength of a given species can simultaneously measure its co-occurrence with its neighbors, and any or all of the biodiversity distances (functional, phylogenetic and taxonomic) with those neighbors (Scheiner, 2012; Vellend et al., 2011; Weiher, 2011; Villéger et al., 2008; Chao et al., 2010). Additionally, centrality measures the structural contribution of the species within the network. Thus, strength connectivity incorporates both the species differences (function, phylogeny, taxonomy) and the topological properties of the network. Next, two measures are defined to quantify species variability over time. The first one, temporal diversity, measures the difference in species proportions across all timestamps. It represents the effective number of species with equal proportions over time. Here, proportions are computed based on strength connectivity. However, the strength connectivity of species may vary from one timestamp to another while the homogeneity of their assemblage remains unchanged. In such cases, temporal diversity will yield the same value as the classical diversity computed on each timestamp (refer to the fourth toy example in Section 2.4.3 for further details). Thus, temporal diversity does not track changes undergone by species across time units as long as the difference between them remains the same. This measure compares only species in the assemblage with each other throughout the timeline, without considering their temporal occurrences. For this reason, a second measure, temporal variation, is proposed to complement the first. It compares each species with its temporal occurrences, and it thus quantifies the homogeneity of their strength connectivity proportions. Thus, the goal is to determine whether species have undergone any changes over time in terms of their strength connectivity. Furthermore, an additional measure is proposed in this work. Its primary purpose is to elucidate the source of diversity changes over time. This measure consists of two distinct components: the first component assesses species composition and turnover, while the second quantifies the differences in strength connectivity between the shared species of two assemblages. These three measures are explained in the following subsections.

The proposed framework is designed to be flexible and applicable to a wide variety of ecological datasets, including terrestrial, freshwater, and marine communities. Below, we detail a step-by-step guide for implementing the framework on any dataset with temporal information on species composition, abundance, biomass, or presence-absence:

- Step 1: Prepare the input data. Collect or organize the data into a matrix format where rows represent sampling units (e.g., sites or time points) and columns represent species. Each cell should contain a measure of species presence, abundance, biomass, or another quantitative value (e.g., density). Temporal information should be associated with each sampling unit to construct a timeline.
- Step 2: Construct the co-occurrence matrix. For each timestamp, compute a pairwise species co-occurrence or similarity matrix. For quantitative data, the 1-Bray-Curtis index is appropriate; for presence-absence data, the 1-Jaccard index. This matrix captures the degree of co-occurrence or association between species at each time point.
- Step 3: Integrate species differences (optional but recommended). If available, build matrices capturing pairwise species differences based on: (i) functional traits (e.g., Gower or Euclidean distances), (ii) phylogenetic relationships (e.g., from molecular phylogenies), or (iii) taxonomic classification (taxonomic rank dissimilarities).
- Step 4: Build temporal networks. For each time point, build a weighted network of species where nodes represent species and edges represent co-occurrence or association strength. Edge weights may be further modified by functional, phylogenetic, or taxonomic distances.
- Step 5: Calculate node strength and connectivity. For each species (node) in each temporal network: (i) compute co-occurrence strength as the sum of edge weights, (ii) optionally integrate functional/phylogenetic/taxonomic strength, (iii) compute degree centrality (normalized) to capture structural position, and (iv) derive the strength connectivity value for each species by combining strength and degree (Eq. (14)).
- Step 6: Compute assemblage strength connectivity (ASC). For each time point, compute the proportion of each species' strength connectivity relative to the sum across all species in the assemblage (Eq. (15)).

- Step 7: Calculate temporal diversity and variation. Using the ASC proportions: temporal diversity (Eq. (19)) measures the effective number of species maintaining consistent structural roles across time, while temporal variation (Eq. (25)) assesses how much the role of each species changes over time.

In addition to these two temporal indices, a third measure can be computed to assess pairwise community dissimilarity between time units, which provides a direct time to time comparison of community states.

2.2. Graph measures

Complex networks or graphs are collections of interconnected entities with a complex internal structure. They are common in both natural and man-made systems, and serve as a fundamental framework for modeling and understanding phenomena across various domains, including ecology (Ghalmane et al., 2020a, 2021, 2022; Al Tfaily et al., 2025; Termos et al., 2023). Various measures provide valuable insights into the properties of a network. Global metrics, such as Density, Transitivity, and Diameter offer information about the overall network structure, while node-specific measures such as Degree and Betweenness centralities, focus on the characteristics of individual nodes within the network. These measures are defined as follows:

2.2.1. Transitivity

The transitivity of the network is its overall probability of having adjacent nodes interconnected. This can be measured using the following equation (Newman, 2018):

$$T = \frac{3 \times \text{number of triangles in the network}}{\text{number of connected triples of nodes in the network}} \tag{1}$$

2.2.2. Density

The density of a network is a measure of how many edges between nodes exist compared to how many edges are possible between the nodes. It is the fraction of the maximum possible number of edges in a network that is actually present. It can be thought of as the probability that a pair of nodes is connected by an edge. It is defined as follows Newman (2018):

$$D = \frac{2E}{N(N-1)} \tag{2}$$

where E is the number of edges in the network and N is the number of nodes in the network.

The links connected to each node play a critical role in determining the node's influence and its overall dynamics within the network. This is why it is essential to measure the network's density to gain a comprehensive understanding of how nodes are interconnected. Its values range from 0 and 1; a higher value indicates that the nodes (species) in the network are strongly interconnected with one another.

2.2.3. Diameter

The diameter (Newman, 2018), d, is defined as the longest of all the shortest paths (geodesics) in the network.

2.2.4. Assortativity

Assortativity (Newman, 2018) in a network refers to the tendency of nodes to connect with other 'similar' nodes over 'dissimilar' nodes. To measure this similarity, Pearson correlation is used between two nodes.

2.2.5. Degree centrality

It is a local, classical centrality measure that quantifies a node's importance by counting the number of its neighbors within a network. It is one of the simplest centralities to compute. Nodes with high Degree centrality have numerous direct connections, highlighting their strong network connectivity and significant role within the network. The Degree centrality C_D of a node i is given by Das et al. (2018):

$$C_D(i) = \frac{d_i}{n-1} \tag{3}$$

where d_i is the number of neighbors of node i in the network and n is the total number of nodes in the network.

2.2.6. Betweenness centrality

It is a global, classical centrality measure that quantifies a node's importance within a network by determining how frequently it appears on the shortest paths between pairs of other nodes. Nodes with high Betweenness centrality serve as a bridges facilitating communication or information flow between different parts of the network. The equation of this centrality is expressed as follows Das et al. (2018):

$$C_B(i) = \sum_{s \neq i \neq t \in V} \frac{\sigma_{st}(i)}{\sigma_{st}} \tag{4}$$

where V is the set of nodes in the graph, σ_{st} is the total number of shortest paths from node s to node t, and $\sigma_{st}(i)$ is the number of shortest paths from s to t that pass through node i. Note that Salathé et al. showed in a previous work (Salathé and Jones, 2010) that local and global measures are strongly correlated when the network is densely connected and has a weak community structure. Hence this justifies the choice of a local measure over a global one.

2.3. Hill numbers

Hill numbers (also called the effective number of species) are a parametric class of diversity measures that incorporates both species richness and proportions. Consider an assemblage containing S species indexed by $i = 1, 2, \ldots, S$, and p_i denotes the relative proportion of the ith species. The Hill numbers equation is defined when $q \neq 1$ as (Hill, 1973):

$$D^q(p) = \left(\sum_{i=1}^{S} p_i^q \right)^{\frac{1}{1-q}}, q \geq 0, q \neq 1 \tag{5}$$

where p_i stands for the proportion of species i. The parameter q refers to the sensitivity of the measure to the relative proportions, as q increases, increasingly more importance is given to the most common or abundant species.

When $q = 0$, Eq. (5) represents simply species richness. It is undefined when $q = 1$, but it is equal to the exponential of the popular Shannon entropy if q tends to 1 (Hill, 1973):

$$D^q(p) = \lim_{q \to 1} D^q(p) = exp\left(\sum_{i=1}^{S} -p_i log(p_i) \right) \tag{6}$$

By using this measure, each species is exactly represented by its relative proportion. When $q = 2$, Eq. (5) is defined as the inverse of Simpson (Hill, 1973):

$$D^2 = \frac{1}{\sum_{i=1}^{S} p_i^2} \tag{7}$$

This diversity measure gives more weight to the species with higher proportions (i.e, more dominant species), and strongly neglects rare species. Generally speaking, the diversity of general order D^q (for all the values of q) represents the effective number of species. It is the number of species that there would be, if all individuals were equally distributed among species (i.e., if they had the same proportion).

True diversity assessed by Hill numbers do not account for the structure of the network of species, even though it is crucial to consider

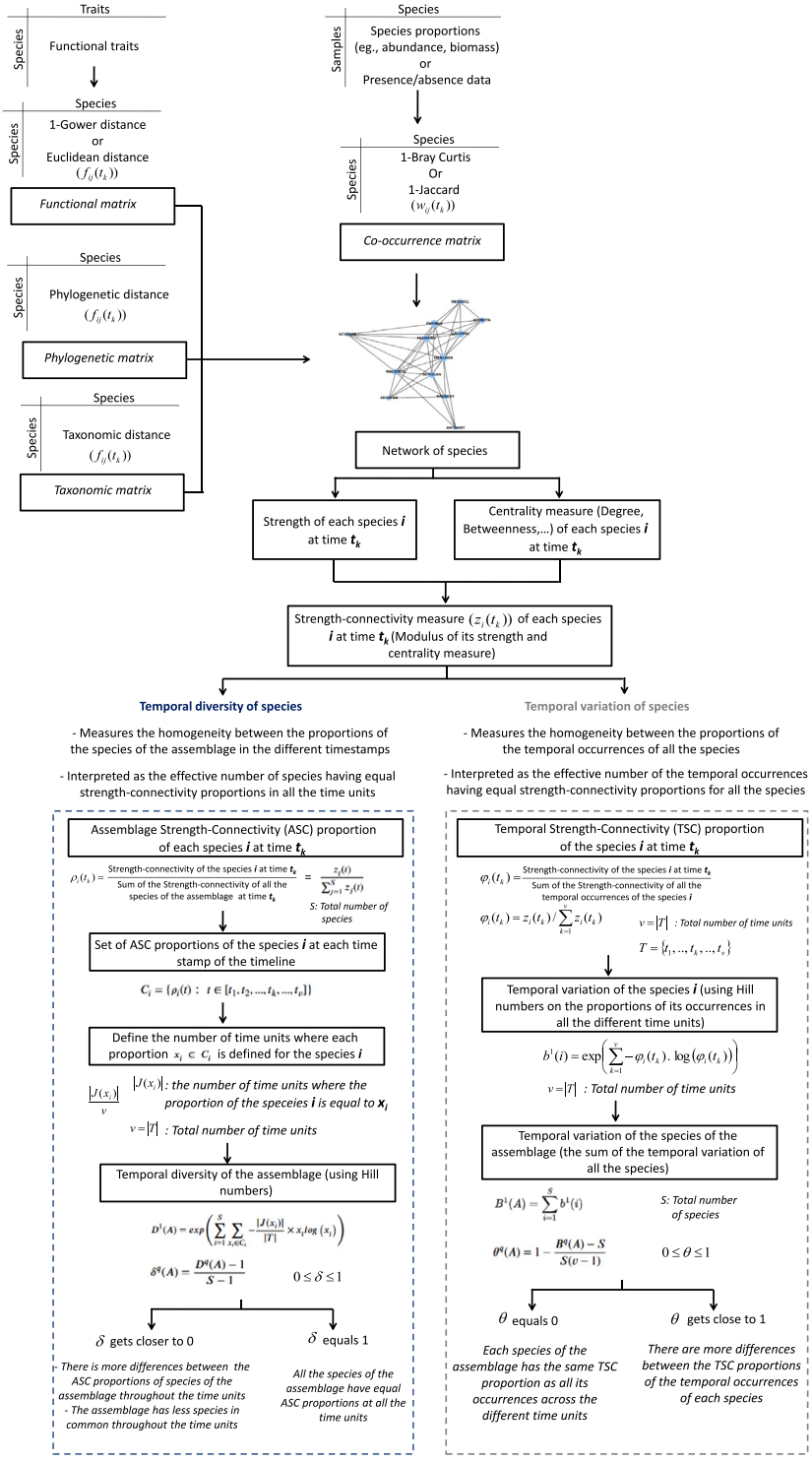

Fig. 1. General scheme of the proposed framework. This workflow illustrates the step-by-step implementation of the framework, from data preparation and network construction to the calculation of temporal diversity and variation measures. Each box represents a key computational step, with arrows indicating the flow of information. The framework is intended for datasets with repeated sampling over time, sufficient replication within each time unit to estimate co-occurrence structure, and consistent sampling design across time steps. In practice, reliable inference typically requires multiple sites or samples per time unit, a sufficient number of time units to characterize trajectories, and an adequate sample size to reduce spurious co-occurrence links. Detailed implementation guidance is provided in Section 2.1.

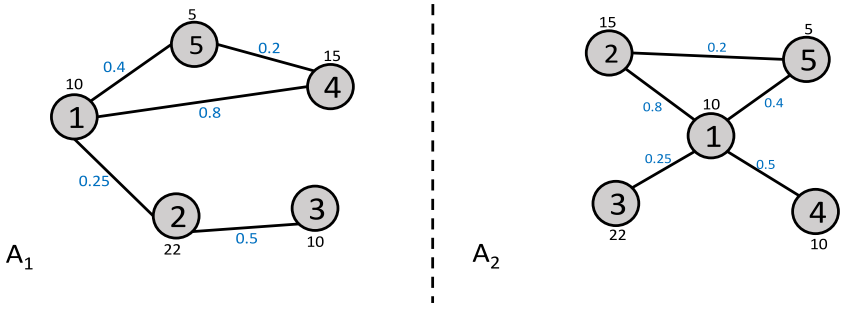

Fig. 2. A toy example of two assemblages A_1 and A_2 with five species each. The weights on nodes represent the abundances of species, while the weights on links (highlighted in blue) represent the co-occurrence frequency of two species. Despite the fact that A_1 and A_2 have different topologies, they have the same species abundance-based diversity $D(A_1) = D(A_2) = 4.49$. They have also the same diversity computed on the probability of associations $D'(A_1) = D'(A_2) = 4.76$. This highlights the importance of considering species network structure when assessing the diversity.

its topology when computing the diversity to differentiate species assemblages (see introduction). For instance, let us assume that the abundance-based diversity of an assemblage A is denoted $D(A)$ (the proportion p of Eq. (5) in this case represents the abundance fraction of each species), while the diversity based on the probability of associations is denoted $D'(A)$ (the proportion p of Eq. (5) in this case represents the probability of association between species). Fig. 2 represents a toy example where both species assemblages A_1 and A_2 have the same values of the diversity computed on the proportion of the abundance of species ($D(A_1) = D(A_2) = 4.49$). The two assemblages also have the same values when the diversity of the probability of associations is computed ($D'(A_1) = D'(A_2) = 4.76$). However, these species assemblages differ entirely in their topological properties. This highlights the importance of considering species network structure when assessing the diversity, an approach that will be introduced in the proposed framework presented in the next subsection.

2.4. Methodological development

Let A be an assemblage of species varying in a timeline $T = \{t_1, t_2, \ldots, t_k, \ldots, t_v\}$, where t stands for a timestamp. The granularity (or resolution) of t may be year, month, week, days, minutes etc. depending of the application. The proposed framework can be, then, applied to the pool of species under study in order to assess its temporal diversity. Its general steps are provided thereafter. All the symbols used in this manuscript are defined in Table 1.

2.4.1. Similarity matrix

The similarity matrix allows to represent an assemblage A of S species. Its elements denotes the similarity or the 1-distance between species, that is to say the differences between them (such as taxonomic, phylogenetic or functional differences). Therefore, different values and indices could be chosen based on the specific objectives of each study and the nature of the available data. For instance about functional diversity, the matrix may represent the functional matrix computed by using the Euclidean distance (for quantitative traits) or the 1-Gower index (mixture of trait types) based on the trait matrix (i.e, species in rows and functional traits in columns). The elements of the similarity matrix may also refer to the similarities between species according to their taxonomic or phylogenetic relatedness, depending on the data available and objectives.

Here, $W_A(t) = [w_{ij}(t)]$ represents the co-occurrence matrix or the Bray-Curtis matrix. $w_{ij}(t)$ is the 1-Bray-Curtis index (Legras et al., 2019b), and represents the probability of association, computed for species pairwise (and not sample pairwise as traditionally used), or co-occurrence frequency between each pair of species i and j at time $t \in T$. The 1-Bray-Curtis index w_{ij} is given as follows:

$$w_{ij}(t) = 1 - \frac{\sum_{k=1}^{u} \left| h_{ik}(t) - h_{jk}(t) \right|}{\sum_{k=1}^{u} h_{ik}(t) + \sum_{k=1}^{u} h_{jk}(t)} \tag{8}$$

Table 1
Names and interpretations of the different symbols used in this manuscript.

Symbol	Name & interpretation
A	Assemblage of species
S	Number of species in the assemblage
T	Set of the timestamps of the assemblage or the timeline
t_k	Timestamp
$A(t_k)$	Assemblage of species at time t_k
h_{ik}	Proportion of the species i (e.g, abundance, biomass, ..) in the sample of species k
W_A	Co-occurrence matrix of the assemblage A (or Bray-Curtis matrix)
w_{ij}	Elements of the co-occurrence matrix computed based on 1-Bray-curtis index between species i and j
F_A	Functional/phylogenetic or taxonomic matrix
f_{ij}	Functional/phylogenetic or taxonomic 1-distance computed between species i and j
a_{ij}	It is equal to 1 when a link exists between nodes i and j (the elements of the adjacency matrix of the network)
m_i	Co-occurrence strength of species i
e_i	Functional/phylogenetic or taxonomic strength of species i
r_i	Strength of species i
d_i	Degree of species i
z_i	Strength connectivity measure of species i
ρ_i	Assemblage Strength connectivity proportion (ASC) of species i
φ_i	Temporal Strength connectivity proportion (TSC) of species i
C_i	Set of the Assemblage Strength connectivity for species i computed on each timestamp
$J(x_i)$	Set of the time units t_k when the proportion x_i is defined ($\rho_i(t_k) = x_i$)
$D^q(A)$	Temporal diversity of general order of an assemblage A
$\delta^q(A)$	Normalized temporal diversity of general order of an assemblage A
$B^q(A)$	Temporal variation of general order of an assemblage A
$\theta^q(A)$	Normalized temporal variation of general order of an assemblage A

where h_{ik} represents the quantity (e.g., abundance, biomass, coverage) of the species i in the sample k, and u is the total number of samples in the assemblage A. In some cases, one can find two species with a high number of occurrences of being seen together but with very small quantities. This is why it is quite important to combine both the frequency of co-occurence and the quantity (proportion) of species. Note that the co-occurrence matrix is used to weight the network of species (so-called the co-occurrence network), where $w_{ij}(t)$ representing the 1-Bray-Curtis, is used as weights of its links at time t.

In this paper, we consider that the matrix $F_A(t) = [f_{ij}(t)]$ denotes the functional/phylogenetic or the taxonomic 1-distance between the species of the assemblage A at time t.

2.4.2. Strength connectivity measure

This new measure is based on the strength and the connectivity of each node (species) of the assemblage. On one hand, connectivity in a network, computed through degree centrality in ecology, primarily reflects the number of relationships each species has within the assemblage. On the other hand, strength represents the sum of the

weights of a node's links, essentially quantifies the overall importance or influence of a species within an assemblage by considering the combined intensity of its relationships with other species. The purpose of this combination is to also introduce the topological structure of the network of species when computing the diversity. This helps prevent the case where two species assemblages exhibit the same diversity but possess a completely different topological structure (as explained before in the toy example given in Fig. 2).

The strength of a node is calculated as the sum of the weights of all its links. The co-occurrence strength of a given node i in a network of species at time t is given by:

$$m_i(t) = \sum_{j=1}^{S} w_{ij}(t) \times a_{ij}(t) \tag{9}$$

where w_{ij} is the co-occurrence frequency of the edge between the species i and j. a_{ij} is equal to 1 when a link between nodes i and j exists. S is the number of species in the assemblage A.

The strength of species can also integrate some or all among-species differences (function, phylogeny and taxonomy). This ensures that the strength of a given species can simultaneously measure the probability of its association with its neighbors (ego network) in terms of co-occurrences (using the Bray Curtis similarity as it is shown in Eq. (9)), functional, phylogenetic, or taxonomic distances with their neighbors. The functional/phylogenetic or taxonomic strength of the species i is defined as:

$$e_i(t) = \sum_{j=1}^{S} f_{ij}(t) \times a_{ij}(t) \tag{10}$$

where f_{ij} is the functional/phylogenetic or taxonomic 1-distance between the species i and j. a_{ij} is equal to 1 when a link between nodes i and j exists, while S is the number of the species in the assemblage A. From the Eqs. (9) and (10) defined above, the total strength of the species i can be defined as follows:

$$r_i(t) = \frac{m_i(t) \times e_i(t)}{\max_{i \in A}(m_i(t) \times e_i(t))} \tag{11}$$

where m_i is the co-occurrence strength, and e_i is the functional/phylogenetic or taxonomic strength of the species i. In cases where the functional, phylogenetic and taxonomic 1-distances are unavailable, the total strength is computed solely based on the co-occurrence strength:

$$r_i(t) = \frac{m_i(t)}{\max_{i \in A}(m_i(t))} \tag{12}$$

The degree of a node i is the number of its connections. The normalized degree is given by:

$$d_i(t) = \frac{\sum_{j=1}^{S} a_{ij}(t)}{S-1} \tag{13}$$

where a_{ij} is equal to 1 when a link between nodes i and j exists, while S is the number of the species.

Finally, based on the previous measures defined in Eqs. (11) and (13), the strength connectivity measure is given by:

$$z_i(t) = \sqrt{r_i(t)^2 + d_i(t)^2} \tag{14}$$

where r_i stands for the strength of species i, and d_i stands for its degree. The strength connectivity z measures both the level of involvement and the connectivity of a node with its neighbors (local network). Note that the level of involvement of a node (species) is expressed by its strength. It is equal to the total sum of the association probabilities with its neighbors, while the connectivity is expressed by the number of its immediate connections or the neighbors (degree).

2.4.3. Temporal diversity of species

a. Definition

First, let us define the Assemblage Strength connectivity proportion (ASC) of each node $i \in A$. It is equal to its strength connectivity divided by the total sum of the strength connectivity of all the nodes of the network (assemblage) A:

$$\rho_i(t) = \frac{z_i(t)}{\sum_{j=1}^{S} z_j(t)} \tag{15}$$

where S is the total number of species in the assemblage. ASC represents the degree to which a species is associated with nearby species in the assemblage.

Then, let us define the set of the strength connectivity proportions ρ_i computed at each timestamp for a given species i. It is given by:

$$C_i = \{\rho_i(t) : \ t \in [t_1, t_2, \ldots, t_k, \ldots, t_v]\} \tag{16}$$

For each element $x_i \in C_i$, the set of its time availability $J(x_i)$ is defined as the set of timestamps t_k where $\rho_i(t_k) = x_i$. It is given by:

$$J(x_i) = \{t_k : \ \rho_i(t_k) = x_i \text{ and } k = 1, 2..., v\} \tag{17}$$

Based on the equations determined in the previous steps, the true temporal diversity of general order $q \neq 1$ for an assemblage A of S species is defined as (Hill, 1973):

$$D^q(A) = \left(\sum_{i=1}^{S} \sum_{x_i \in C_i} \frac{|J(x_i)|}{|T|} \times (x_i)^q \right)^{\frac{1}{1-q}} \tag{18}$$

where S_i is the set of the strength connectivity of the species i defined in the different timestamps. $|J(x_i)|$ represents the number of timestamps where the strength connectivity of species i is equal to $x_i \in S_i$. $|T|$ represents the total number of timestamps in the timeline.

The true temporal diversity ranges between 1 and S (the number of species in the assemblage, see Table 1). For a general order of q, the true temporal diversity is interpreted as the effective number of species having equal ASC proportions in all timestamps. In other terms, if $D^q(A) = y$, then the diversity of the assemblage A is the same as that of an idealized assemblage with y species, all of equal ASC probabilities across all timestamps. The true temporal diversity measures the number of species that would have an equal influence within its community across all timestamps. This helps us understand how diverse the species are in terms of their temporal distribution.

This measure can be normalized and represented as a dissimilarity measure as follows:

$$\delta^q(A) = \frac{D^q(A) - 1}{S - 1} \tag{19}$$

This measure ranges between 0 and 1. It is equal to 1 if all the species of the assemblage have equal ASC proportions across all time units. Note that this measure could be applied to the simpler case where there is only one timestamp. In this case, the set of the strength connectivity proportions (Eq. (16)) will contain only one element. It can be noticed that the final equation of the temporal diversity index is formulated in terms of individual species rather than all pairs of species. However, these pairwise relationships are considered by mean of the Bray-Curtis dissimilarity (Eq. (8)), and especially in the equation of the Strength-Connectivity measure (Eq. (15)) which considers the relationship of each species with the other species of the assemblage.

The Eq. (18) is undefined for $q = 1$, but as q tends to 1, its limit is equal to Hill (1973):

$$D^1(A) = exp\left(\sum_{i=1}^{S} \sum_{x_i \in C_i} -\frac{|J(x_i)|}{|T|} \times x_i log\left(x_i\right) \right) \tag{20}$$

where q is a parameter that modulates the weight given to strength connectivity proportion of species. If $q = 1$, each species is exactly weighted by its proportional strength connectivity. When $q > 1$, the weight given to species with high strength connectivity proportion is preponderant, and when $q < 1$, more weight is given to species with low strength connectivity. The temporal diversity tracks the changes that may affect the topology of the local network of nodes across different timestamps. The local network of a node is formed by its neighbors (also referred to as the ego network).

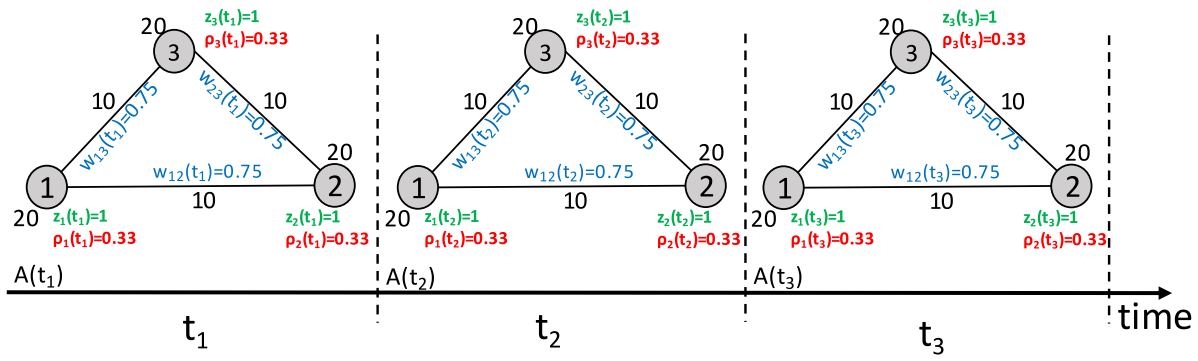

Fig. 3. A toy example of an assemblage A that varies in three timestamps t_1, t_2 and t_3. The weights on nodes (in black) represent the abundances of species 1, 2, 3 (circle or node), while the weights on links (in black) represent the number of times they co-occure in all the samples. The values in blue (w_{ij}) represent the weights of the links computed based on the 1-Bray-Curtis index, the values in green (z_i) represent the strength connectivity of the nodes, while those highlighted in red (ρ_i) represent the values of their Assemblage Strength Connectivity proportions. The temporal diversity of this assemblage is equal to $D^q(A) = 3$.

b. Toy example

To illustrate the definition of temporal diversity, let us consider the example of an assemblage A of three species that varies across three timestamps (Fig. 3). In this example, the species have the same co-occurrence frequency with each other $w_{12}(t_1) = w_{23}(t_1) = w_{13}(t_1) = 1 - (10/(20+20)) = 0.75$, as well as the same strength $m_1(t_1) = w_{12}(t_1) + w_{13}(t_1) = 0.75 + 0.75 = 1.5 = m_2(t_1) = m_3(t_1)$, Then, they also have the same normalized strength $r_1(t_1) = 1 = r_2(t_1) = r_3(t_1)$. Additionally, they have the same number of connections, their normalized degree is $d_1(t_1) = d_2(t_1) = d_3(t_1) = 2/2 = 1$. Therefore, they have an equal strength connectivity $z_1(t_1) = 1 = z_2(t_1) = z_3(t_1)$. The ASC is then equal to $\rho_1(t_1) = 1/3 = \rho_2(t_1) = \rho_3(t_1)$. The values of all these parameters do not change in the other timestamps (t_2 and t_3). Thus, the sets of the strength connectivity proportions of the three nodes are $C_1 = C_2 = C_3 = \{1/3\}$. Additionally, $|J(1/3)|/|T| = 3/3 = 1$ since all the nodes have the same strength connectivity across timestamps.

Therefore, according to the Eqs. (18) and (19), the temporal diversity of this assemblage A ($D^q(A) = 3$ and $\delta^q(A) = 1$) is the same as that of an idealized assemblage with 3 species all of equal strength connectivity proportions ($\rho_1(t) = \rho_2(t) = \rho_3(t) = 1/3$). Note that more examples with alternate scenarios are available in the supplementary materials to better detail the definition of temporal diversity.

2.4.4. Temporal variation of species

a. Definition

The previous measure highlights the differences between the proportions of species of the assemblage in the various timestamps. However, as shown in the toy example provided in the Appendix (Fig. A.1, Table A.1), the proportions can increase for some species between the first timestamp and the second one while it has decreased for some others. Yet, Temporal diversity has the same value as the classical diversity computed on both timestamps. This is because the homogeneity between the proportions of the species in the assemblage was preserved across both timestamps. Thus, Temporal diversity compares only species with each other without considering the comparison of their proportions with their respective temporal occurrences. In other words, it does not track their variation across timestamps. To solve this issue, the concept of "Temporal variation" is introduced in this section to complement Temporal diversity. This measure assesses fluctuation in the species' strength connectivity over time.

To define Temporal variation, let us define at first the Temporal Strength Connectivity proportion (TSC). TSC φ_i of species i is given as follows:

$$\varphi_i(t_k) = \frac{z_i(t_k)}{\sum_{k=1}^{v} z_j(t_k)} \tag{21}$$

where z_i is the strength connectivity of the species, and v is the total number of the time units. The temporal variation of species does not require comparing them with one another, but rather quantifies the extent to which they have changed over time in terms of strength connectivity. It can be defined for a species i of the assemblage as follows:

$$b^q(i) = \left(\sum_{k=1}^{v} \varphi_i(t_k)^q \right)^{\frac{1}{1-q}} \tag{22}$$

where v is the number of the time units, and φ_i is the TSC of species i. When $q = 1$, the new measure is defined as:

$$b^1(i) = exp\left(\sum_{k=1}^{v} -\varphi_i(t_k) \times log\left(\varphi_i(t_k)\right) \right) \tag{23}$$

Therefore, the temporal variation for an assemblage of species A is then defined as:

$$B^q(A) = \sum_{i=1}^{S} b^q(i) \tag{24}$$

where S is the number of species in the assemblage A. This measure ranges between S and $S * v$. It is interpreted as the effective number of the temporal occurrences of all the species having equal TSC proportions. It measures the amount of fluctuation each species' Strength connectivity has undergone across timestamps, helping to assess community diversity over time. The normalized temporal variation measure θ is represented as follows:

$$\theta^q(A) = 1 - \frac{B^q(A) - S}{S(v-1)} \tag{25}$$

This measure ranges between 0 and 1. It is close to 1 if there are bigger differences between the TSC proportions of the temporal occurrences of all the species. In that case, the species of the assemblage have undergone a huge change in terms of their Strength connectivity.

b. Toy examples

Fig. 4 illustrates a toy example (similar to the last toy example presented in the supplementary materials), where species have different strength connectivity values in two timestamps. Yet, their diversity in the timestamps has the same value as their temporal diversity ($D^1(A) = D^1(A(t_1)) = D^1(A(t_2))$). Species 1 have different strength in the two timestamps $m_1(t_1) = 0.1$ and $m_1(t_2) = 2.93$, while its normalized strength is $r_1(t_1) = 0.034$ and $r_1(t_2) = 1$. They also have different number of connections $d_1(t_1) = 2/4 = 0.5$ and $d_1(t_2) = 4/4 = 1$. Therefore, the strength connectivity changes between the two timestamps: $z_1(t_1) = 0.5$ and $z_1(t_2) = 1.41$. TSC of the species 1 is $\varphi_1(t_1) = 0.27$ and $\varphi_1(t_2) = 0.73$. Proportions are computed in the same way for all the other species of the assemblage. In this case, temporal variation is $B^1(A) = 9.41$ (Eq. (24)), and the normalized measure is $\theta^1(A) = 0.12$ (Eq. (25)).

It is observeded that the value of temporal variation differs from the diversity computed in each timestamp. This is because this measure accounts for the differences in how the same species appear across

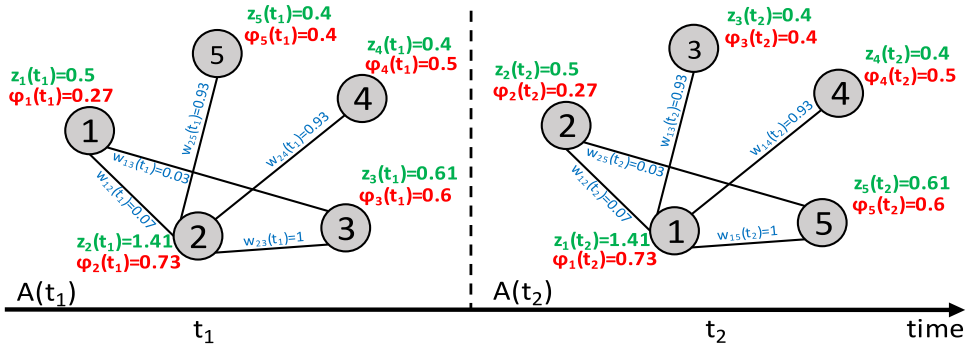

Fig. 4. A toy example of an assemblage A that varies in two timestamps t_1 and t_2. The values in blue (w_{ij}) represent the weights of the links or the co-occurrence frequency computed based on the 1-Bray-Curtis index, the values in green (z_i) represent the strength connectivity of the nodes, while those highlighted in red (φ_i) represent the values of their Temporal Strength connectivity proportions. The normalized temporal variation of this assemblage is equal to $\theta^1(A) = 0.12$.

various timestamps. Additionally, the value of its normalized version is relatively low ($\theta^1(A) = 0.12$). This is due to the fact that only species 1, 2, and 3 experience important changes in terms of the strength connectivity proportions over time, while the proportions of other species have changed only slightly ($\varphi_1(t_1) = 0.27$ and $\varphi_1(t_2) = 0.73$, $\varphi_2(t_1) = 0.73$ and $\varphi_2(t_2) = 0.27$, $\varphi_3(t_1) = 0.6$ and $\varphi_3(t_2) = 0.4$, $\varphi_4(t_1) = 0.5$ and $\varphi_4(t_2) = 0.5$, $\varphi_5(t_1) = 0.4$ and $\varphi_5(t_2) = 0.6$).

2.4.5. Pairwise community dissimilarity

In this subsection, we extend the framework by introducing indices that allow us to delve deeper into understanding the origin of these changes. Specifically, these indices help distinguish whether the observed temporal change stems from shifts in species composition or from alterations in how the overlapping species within these assemblages are interconnected. This additional layer of analysis enhances our understanding of the mechanisms driving temporal diversity changes. Previous works (Poisot et al., 2012; Poisot, 2022; CaraDonna et al., 2017) proposed and applied an approach to assess the differences among species of two networks (assemblages) based on the β_{WN} index. It encompassed two additive components assessed by two complementary indices. The first component (β_{ST}) quantifies the dissimilarity in species composition or species turnover. Indeed, through time or space, some species could appear or disappear (or not be sampled) which could cause the loss or gain of some species' differences among the two assemblages. Moreover, since the species shared between two assemblages may be related differently, the second component (β_{OS}) allows for assessing the change in how the overlapping species of these assemblages are connected or linked (e.g. the appearance or disappearance of a connection). Note that as mentioned in the introduction, the connection refers here to the pairwise difference between species. Thus, the dissimilarity between two networks is:

$$\beta_{WN} = \beta_{ST} + \beta_{OS} \tag{26}$$

Poisot et al. (2012) also used the approach put forth by Koleff et al. (2003) to measure network dissimilarity. This method relies on a reformulation of the conventional dissimilarity indices, which consists of a partition of shared and total species. It divides the differences found in two assemblages X and Y into three sets for which their cardinality (a, b and c) is computed. The dissimilarity index is given by the following formula:

$$\beta_W = \frac{a + b + c}{(2a + b + c)/2} - 1 \tag{27}$$

where a counts the number of shared elements (i.e., number of links) between the sets X and Y (i.e., $a = \|X \cap Y\|$), b counts the number of links found only in the set X (i.e., $b = \|X \setminus Y\|$), and c counts the number of links found only in the set Y (i.e., $c = \|Y \setminus X\|$). Note that β_W is used to compute both β_{OS} (the pairwise dissimilarity of the shared species) and β_{WN} (the pairwise dissimilarity of the whole networks or assemblages), as illustrated below. Additionally, the value of β_{ST} is derived from Eq. (26).

If we consider the assemblages (networks) X and Y illustrated in Fig. A.1, we can easily compute their dissimilarity using these measures. Note that for the first example below, pairwise differences' values (in blue, Fig. A.1) are not considered, but only the link structure among species (i.e., topological structure). This structure represents species co-occurrence (based on species presence-absence data, or quantitative data (e.g., species abundance, biomass, or coverage)). It is noticed from the toy example that the two assemblages share some species, with similar link structure (i.e., species 1, 2, 3 and 4). However, assemblages X and Y differ in that X has one more species than Y (species 5). Let us start by computing β_{OS}; it is noticed that the shared species have exactly the same link structure. Thus, $\beta_{OS} = \beta_W([a = 3, b = 0, c = 0]) = 0$ meaning that there is no difference in link structure between the shared species. On the other hand, looking at the whole network, assemblage X has two more links than assemblage Y due to the presence of species 5. Thus, $\beta_{WN} = \beta_W([a = 3, b = 2, c = 0]) = 0.25$. Based on Eq. (26), $\beta_{ST} = \beta_{WN} - \beta_{OS} = 0.25$. Therefore, the dissimilarity between assemblages X and Y is explained only by the difference in species composition ($\beta_{ST} = 0.25$ and $\beta_{OS} = 0$). Indeed, there are no link structure differences for the shared species, but the absence of species 5 in network Y causes the dissimilarity between the assemblages. Based on this example, we can notice that the species shared between assemblages X and Y have the same topological structure ($\beta_{OS} = 0$).

In addition to the method proposed by Poisot et al. (2012) and Poisot (2022), it is possible to consider the degree of relatedness among species commonly used in community diversity analyses (e.g., functional, phylogeny, taxonomy distances, blue values in Fig. A.1). Indeed, despite the fact that species may have quite similar network structure, they may have totally different functional, taxonomic or phylogenetic differences. In other terms, species may have totally different strengths. This could be quantified by using the strength connectivity measure proposed in our framework. The latter is based on a combination of the degree centrality quantifying the structural position of each species in the assemblage, and the strength quantifying the functional, phylogenetic or taxonomic pairwise distances between species and their local neighborhood in the assemblage. Therefore, it is very important to use this information on species differences while computing the whole network dissimilarity measure β_{WN}. In this context, our proposed framework includes the approach proposed by Poisot et al. (2012) and Poisot (2022), consisting of the above two additive components (β_{OS} and β_{ST}), and extends it by using the following dissimilarity measure between two assemblages:

$$\beta_Z = \frac{e + f + g}{(2e + f + g)/2} - 1 \tag{28}$$

where e counts the number of species having the same strength connectivity for the shared species of the assemblages X and Y; f counts the

number of species found in X with a different strength connectivity than Y, while g is the number of species found in Y with a different strength connectivity than X. Similarly to the previous measure, β_z is used to compute β_{OS} and β_{WN} while β_{ST} could be derived according to Eq. (26). Let us examine again the toy example in Fig. A.1, this time by considering also the species differences (values in blue), such as functional (phylogenetic or taxonomic) distances between species. As previously mentioned, shared species between the two assemblages have similar local topological structure. Yet, species have different functional distances. Hence they also have different strength connectivity (except for species 1 which has the same strength connectivity in both assemblages, refer to Table A.1 for all the strength connectivity values). If we consider first the species shared between assemblages X and Y, only species 1 has the same strength connectivity in both assemblages (SC = 1.41, Table A.1), thus $e = 1$. In contrast, the three other shared species 2, 3, 4 have different values from one assemblage to the other (Table A.1), thus $f = 3$ and $g = 0$. Thus, $\beta_{OS} = \beta_Z([e = 1, f = 3, g = 0]) = 0.6$. Considering the whole two networks, i.e., not only shared species, species 5 is present only in assemblage X. Thus, $\beta_{WN} = \beta_Z([a = 1, b = 4, c = 0]) = 0.7$. Based on Eq. (26), $\beta_{ST} = \beta_{WN} - \beta_{OS} = 0.1$. β_{OS} and β_{ST} are both different from 0, therefore the dissimilarity between the assemblages X and Y is explained first by the functional difference between the shared species ($\beta_{OS} = 0.6$) and to a lesser extent by species turnover $\beta_{ST} = 0.1$. On one hand, there are high functional pairwise distances between the shared species among X and Y ($\beta_{OS} = 0.6$), explained by the fact that the three shared species have different strength connectivity values in both assemblages (due to their different functional distances with the other species belonging to their local neighborhood). On the other hand, the species composition also leads to this functional difference between the two assemblages due to the presence of species 5 only in assemblage X.

2.4.6. Summary

To summarize, the proposed framework comprises three diversity measures (Eqs. (19), (25) and (26)). They integrate the local strength of a species with its neighbors (Formula (9)) and assess its local or global influence using centrality measures. The framework is designed to offer flexibility in utilizing various centrality measures depending on the network structure. In this context, we exclusively consider the degree (or connectivity) of species, defined as the number of their connections, since it represents a widely used metric for capturing local network features. Furthermore, for dense networks, such as the species networks utilized in this study, global measures (e.g., betweenness centrality) exhibit strong correlations with local measures, supporting our decision to focus solely on local measures. Additionally, local measures such as the degree are more computationally efficient compared to global measures.

In the proposed framework, while we emphasize the temporal dynamics of community diversity, it is essential to highlight the importance of spatial resolution/scale in understanding ecological patterns and processes. This framework ensures flexibility, allowing users to consider spatial information according to their specific research questions and objectives. The spatial resolution or sampling unit can vary depending on the study, ranging from fine-scale localized sampling to broader regional or global assessments.

2.5. Data sets

2.5.1. Case study 1

Species abundance data was sampled from more than 20,000 km of coastline by the MEDITS 'Mediterranean international trawl survey' between 1994 and 2019 according to a standardized protocol [see for details Bertrand et al., 2002; Spedicato et al., 2019]. This program is funded annually by the European Commission within the Data Collection Framework (DCF), from 2003 until at least 2027 (obligatory in the frame of the EU Common Fisheries Policy (CFP)). The hauling depth goes down to 800 m, and the study area ranges from 34.33°N to 45.67°N and 5.22°W to 34.09°E, and was divided into 18 operative Geographical Sub-Areas (GSAs) defined by the General Fisheries Commission for the Mediterranean Sea (Fig. 5). Overall, during the studied period, a total of about 18,000 hauls were sampled, and 154 different species were collected. Eight explanatory variables were also considered. Seven variables are related to the environment (depth, temperature, chlorophyll-a concentration, salinity, phosphate, nitrate and phytoplankton carbon biomass 'Pcb') and one is related to the fishing pressure (see Mérigot et al. (2019) for more details regarding these variables). Before applying the framework, the density matrix (i.e., hauls × species density of each species) was computed based on the abundance data collected divided by the swept area of each haul. Then, the creation of a network for each of the seventeen GSAs and their characterization using graph measures presented in Section 2.2 were first implemented. Second, the different steps of the proposed approach, presented above in Section 2.1, were applied to compute the temporal diversity as well as the temporal variation of the nine GSAs that were covered over the whole timeline ranging from the year 1994 to 2019.

2.5.2. Case study 2

The proposed framework is also applied to a bat dataset collected in Central Amazonia, Brazil, over four years (2011, 2012, 2013 and 2014, Farneda et al. (2015)). The study area consists of 8 fragments of different sizes: three 1 ha fragments, three 10 ha fragments and two 100 ha fragments. They were isolated from the continuous forest by distances of 80–650 m due to various factors such as burning of the surrounding forest. Bats were captured at different sites located 100 m from one of the boundaries of each fragment. A similar sampling scheme was applied in the continuous forest. Overall, a total of 39 sites were sampled, and 41 different species were collected.

3. Results

3.1. Case study 1

First of all, the networks of the different GSAs were formed in order to use information regarding their topological structure while assessing their species diversity. Each network is composed of a set of nodes (species) and links (between two species collected in the same haul). The example of the network of GSA 1 is given in Figure S5. Then, the links were weighted by the elements of one of the distance matrices (co-occurrence, functional, phylogenetic or taxonomic). Networks had different sizes ranging from 39 nodes in GSA 2 (GSA with the lowest number of species in terms of γ-diversity) to 100 nodes found in the network of GSA 9 (highest number of species in terms of γ-diversity). To assess networks, density, diameter, transitivity and assortativity were also computed (see Section 2.2). As expected from co-occurrence data, networks had high density Table 2, with nodes tightly connected to each other. This network structure justifies our use of local centrality measures (degree) rather than global measures, as the two are strongly correlated in dense networks (Salathé and Jones, 2010). Additionally, all networks had small diameters, high transitivity and negative assortativity.

The two global measures, temporal diversity δ and temporal variation θ, were computed for each GSA, and a k-means method was used to classify them according to these two overall measures. GSAs exhibit different patterns, and were grouped into five clusters (Fig. 6), determined using the elbow method to determine the optimal number of clusters in k-means by plotting the within-cluster sum of squares against the number of clusters and identifying the "elbow" point where the rate of decrease sharply slows (Fig. 7): cluster 1: GSAs 1 and 17; cluster 2: GSAs 16 and 18; cluster 3: GSAs 19 and 6; cluster 4: GSAs 9 and 11; cluster 5: GSA 7. This result highlights that many GSAs exhibit similar patterns, even though they are in completely different geographical

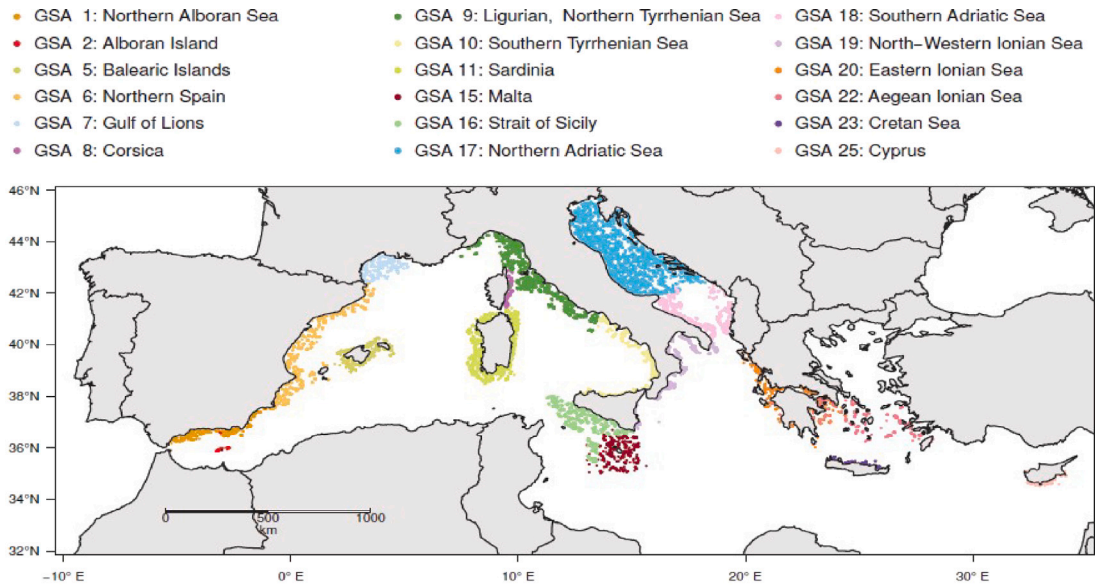

Fig. 5. Studied area, northern Mediterranean sea. Each point represents a haul (i.e., sample) performed in the frame of the european MEDITS program based on standardized scientific surveys.

Table 2
The mean and standard deviation values of the main properties of the network for the different Geographical Sub-Areas (GSAs) computed all over the years under study. n and m are respectively the size of the network and the number of its edges. e is the diameter. μ represents the density of the network. t is the transitivity while σ is the assortativity of the network. Only the nine first GSAs having the same time coverage (1994–2019) are comparable and considered in this table.

Network	Years of study	n	m	e	μ	t	σ
GSA 1	1994–2019	82.65 ± 7.43	1564.81 ± 296.9	2.88 ± 0.33	0.46 ± 0.04	0.69 ± 0.02	−0.16 ± 0.03
GSA 6	1994–2019	82.42 ± 5.63	1588.27 ± 285.74	3 ± 0.0	0.47 ± 0.04	0.7 ± 0.03	−0.12 ± 0.04
GSA 7	1994–2019	51.23 ± 3.63	700.35 ± 82.75	2.69 ± 0.47	0.54 ± 0.04	0.73 ± 0.02	−0.16 ± 0.04
GSA 9	1994–2019	100.12 ± 3.7	2147.46 ± 137.27	2.96 ± 0.2	0.43 ± 0.03	0.67 ± 0.02	−0.15 ± 0.02
GSA 11	1994–2019	91.65 ± 3.3	2044.04 ± 219.05	3 ± 0.0	0.49 ± 0.03	0.71 ± 0.02	−0.09 ± 0.03
GSA 16	1994–2019	91.54 ± 9.8	1952.92 ± 472.88	2.92 ± 0.27	0.46 ± 0.04	0.69 ± 0.02	−0.15 ± 0.02
GSA 17	1994–2019	81.04 ± 6.54	1686.88 ± 315.02	2.81 ± 0.4	0.51 ± 0.05	0.72 ± 0.03	−0.18 ± 0.06
GSA 18	1994–2019	91.5 ± 7.38	2599.62 ± 654.76	2.31 ± 0.47	0.62 ± 0.1	0.77 ± 0.06	−0.22 ± 0.06
GSA 19	1994–2019	79.08 ± 7.69	1309.38 ± 238.06	3 ± 0.0	0.42 ± 0.04	0.66 ± 0.03	−0.14 ± 0.05
GSA 2	1994, 1999–2000, 2005–2009, 2011–2019	39 ± 12.03	449.12 ± 179.15	2.35 ± 0.7	0.63 ± 0.19	0.83 ± 0.08	–
GSA 5	2001–2019	53.26 ± 10.9	579.74 ± 330.08	3.58 ± 0.69	0.39 ± 0.05	0.69 ± 0.02	−0.09 ± 0.04
GSA 10	1994–2016	89.87 ± 8.7	2559.43 ± 647.16	2.57 ± 0.59	0.63 ± 0.11	0.78 ± 0.06	−0.22 ± 0.04
GSA 15	2002–2019	80.67 ± 6.97	1534.11 ± 287.44	2.89 ± 0.32	0.47 ± 0.03	0.7 ± 0.02	−0.15 ± 0.02
GSA 20	1994–2001, 2003–2006, 2008, 2014, 2016, 2018–2019	90.18 ± 15.56	1983.12 ± 608.9	2.94 ± 0.24	0.47 ± 0.04	0.71 ± 0.02	−0.13 ± 0.03
GSA 22	1994–1995, 1998–2001, 2003–2006, 2008, 2014, 2016, 2018–2019	68.6 ± 21.17	1250.1 ± 568.53	3 ± 0.0	0.52 ± 0.07	0.72 ± 0.04	−0.12 ± 0.05
GSA 23	1994, 1996, 2004–2006, 2008, 2014, 2016, 2018–2019	53 ± 16.32	754 ± 360.83	3 ± 0.0	0.52 ± 0.07	0.73 ± 0.03	−0.09 ± 0.06
GSA 25	2005–2015, 2017–2019	64.62 ± 6.1	907.46 ± 192.81	3.08 ± 0.28	0.44 ± 0.04	0.73 ± 0.02	0

locations and vice versa. For instance, GSA 7 (Gulf of Lions) has the lowest temporal diversity, while GSA 9 (Ligurian, Northern Tyrrhenian sea) has the highest value, even though GSAs 7 and 9 are located next to each other.

The results also showed that the GSAs exhibit the same pattern after computing the temporal diversity and temporal variation while considering the different distances between species (function, phylogeny and taxonomy). This is due to the fact that the co-occurrence, functional, phylogenetic and taxonomic networks are quite similar. To state this result, two complementary analyses were conducted. The first analysis aimed to assess the similarity between the four networks in terms of their most connected nodes, defined by their weighted

Table 3
Results of the temporal diversity and the Temporal variation of species computed on the bat species assemblages sampled in the Amazonian forest in Brazil.

Habitat	Temporal diversity	Temporal variation of species
1 ha fragments	0.21	0.85
10 ha fragments	0.31	0.76
100 ha fragments	0.37	0.69
Continuous forest	0.56	0.46

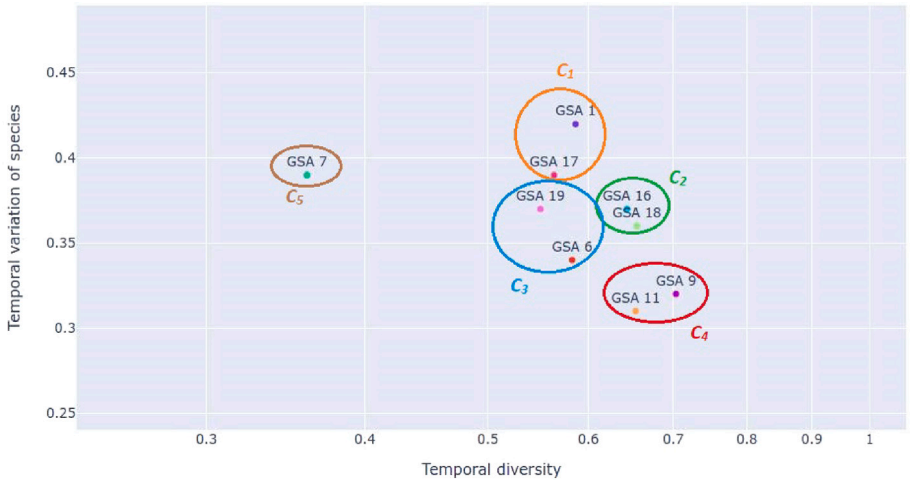

Fig. 6. Temporal variation and temporal diversity of the various Geographical Sub-Areas (GSAs). They are clustered into 5 groups by using the k-means method.

Table 4
The mean and standard deviation values of the proportion of the overlap between the sets of the 20 most connected nodes according to the weighted degree. The nodes are selected from the co-occurrence, functional, phylogenetic and taxonomic networks. The proportion of the overlap is computed by using the jaccard index all over the years studied (1994–2019).

	Co-occurrence VS. Function	Co-occurrence VS. Taxonomy	Co-occurrence VS. Phylogeny
GSA 1	66.67 ± 3.03	65.67 ± 6,45	59.89 ± 5.38
GSA 6	71.96 ± 7.56	72.3 ± 7,12	70.48 ± 9.05
GSA 7	65.18 ± 6.06	66.05 ± 7.37	68.14 ± 9.58
GSA 9	70.46 ± 6.63	73.18 ± 8.13	72.59 ± 8.19
GSA 11	64.95 ± 7.37	68.23 ± 6	61.99 ± 5.46
GSA 16	66.97 ± 6.18	69.92 ± 8.08	57.22 ± 6.35
GSA 17	66.97 ± 7.41	71.78 ± 9.57	65.98 ± 8.37
GSA 18	72.05 ± 7.8	71.64 ± 7.75	70.55 ± 7.84
GSA 19	66.87 ± 5.51	62.35 ± 6.92	56.71 ± 5.79

Table 5
Results of the comparison between the evolution of the different networks formed in the GSA 19. Pearson correlation is computed between their sets of the proportion of the overlap. The proportion of the overlap is computed by using the jaccard index between the sets of the highly connected nodes found in two consecutive years.

	Co-occurrence	Function	Taxonomy	Phylogeny
Co-occurrence	1	0.94	0.95	0.88
Function	0.94	1	0.96	0.92
Taxonomy	0.95	0.96	1	0.91
Phylogeny	0.88	0.92	0.91	1

degree (Opsahl et al., 2010). Using the Jaccard index, we measured the overlap between the sets of top nodes (those with the highest weighted degree) in each network. As shown in Table 4, the Jaccard index values are consistently high, indicating that the same nodes tend to be highly connected across all four networks. Additionally, the second analysis examined the patterns of change in the four networks for each GSA. To do so, the networks formed in two consecutive years were compared by computing the proportion of the overlap between their sets of the top connected nodes (using the Jaccard index). Then, the sets of the proportion of the overlap are defined for the four networks representing their evolution. After that, Pearson correlation coefficient was computed between these sets (Table 5). The results showed that the values of the correlation coefficient are very high (close to 1). Therefore, all four networks had about the same pattern of change in the period between 1994 and 2019.

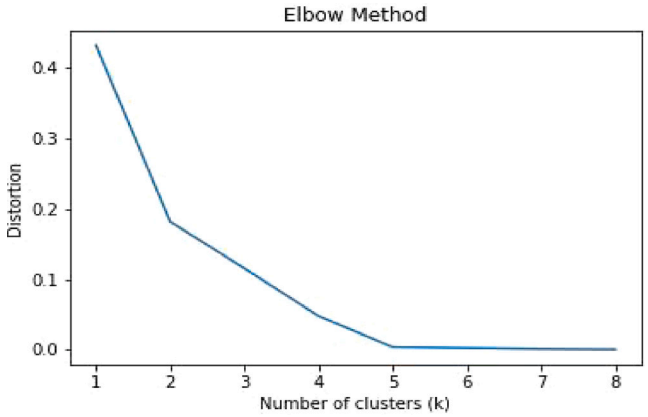

Fig. 7. Graphic of the elbow method used to choose the number of clusters.

To explain the above patterns, a complementary analysis revealed the influence of environmental and fishing variables on temporal diversity across different GSAs (Tables 6–19). Depth consistently emerged as a key factor shaping diversity due to its role in structuring demersal fish communities. Other influencing variables varied according to clusters: in Cluster 1, Pcb and Chlorophyll negatively impacted diversity. In Cluster 2, Nitrate and FPI were the most influential variables, with a similar negative effect on diversity, while Depth had varying impacts. In Cluster 3, Nitrate, Temperature, and FPI were the main drivers, all negatively affecting diversity. In Clusters 4 and 5, the impact of environmental variables was moderate, with Phosphate, Pcb, and Chlorophyll contributing less significantly. These findings demonstrate shared patterns within clusters while also highlighting variability in the drivers of diversity across GSAs. For visualization purposes, the evolution of GSA 1 throughout time is illustrated in Fig. 8. The classification of GSA 1 as the area with the highest degree of major change in species strength connectivity is visually supported by this figure, which depicts the network structure across 1994, 2005, and 2010. The high Temporal Variation (θ) calculated by our framework is manifested in the figure through clear topological rewiring and structural turnover observed between the three time periods. This comparative visualization highlights that the identity and connections of central 'hub' species undergo significant shifts, providing compelling visual evidence for the dynamic nature and instability of the GSA 1 ecological network over time.

Table 6
Results of the multiple linear regression performed on the temporal diversity of the GSAs belonging to the cluster 1. The explanatory variables are sorted according to their influence. The variables having high impact on diversity have a coefficient significantly different from 0.

Impact on diversity	GSA 1			GSA 17		
	Env. variables	Coef	R^2	Env. variables	Coef	R^2
High	Phosphate	−0.423	0.431	Chlorophyll	−0.768	0.578
	Chlorophyll	−0.423		Pcb (highly correlated with Chlorophyll)	–	
	Pcb (highly correlated with Chlorophyll)	–		Salinity	−0.262	
	Salinity	0.173		Phosphate	0.18	
Low	Nitrate (correlated with Phosphate)			Nitrate (correlated with Phosphate)		
No impact	Depth			Depth		
	Temperature			Temperature		
	FPI			FPI		

Table 7
Results of the multiple linear regression performed on the temporal diversity of the GSAs belonging to the cluster 2. The explanatory variables are sorted according to their influence. The variables having high impact on diversity have a coefficient significantly different from 0.

Impact on diversity	GSA 16			GSA 18		
	Env. variables	Coef	R^2	Env. variables	Coef	R^2
High	Nitrate	−0.66	0.393	Nitrate	−0.54	0.354
	FPI (highly correlated with Nitrate)	–		FPI (highly correlated with Nitrate)	–	
	Phosphate (highly correlated with Nitrate)	–		Chlorophyll (correlated with Nitrate)	–	
	Chlorophyll (negatively correlated with Nitrate)	–		Temperature (negatively correlated with Nitrate)	–	
	Salinity (negatively correlated with Nitrate)	–		Depth	0.45	
	Depth	−0.41		Salinity	−0.11	
Low	Temperature (correlated with Nitrate)	–		Phosphate (negatively correlated with Nitrate)	–	
No impact	Pcb			Pcb		

Table 8
Results of the multiple linear regression performed on the temporal diversity of the GSAs belonging to the cluster 3. The explanatory variables are sorted according to their influence. The variables having high impact on diversity have a coefficient significantly different from 0.

Impact on diversity	GSA 11			GSA 9		
	Env. variables	Coef	R^2	Env. variables	Coef	R^2
High	Pcb	−1.01	0.5	Temperature	−0.264	0.244
	Chlorophyll (highly correlated with Pcb)	–		Nitrate	−0.217	
	Temperature	−0.58		FPI (correlated with Nitrate)	–	
	Salinity (correlated with Temperature)	–		Phosphate (correlated with Nitrate)	–	
	FPI	−0.18		Pcb	0.215	
	Nitrate (correlated with FPI)	–				
Low	Phosphate	−0.074		Salinity	0.09	
No impact	Depth			Depth		
				Chlorophyll		

Table 9
Results of the multiple linear regression performed on the temporal diversity of the GSAs belonging to the cluster 4. The explanatory variables are sorted according to their influence. The variables having high impact on diversity have a coefficient significantly different from 0.

Impact on diversity	GSA 6			GSA 19		
	Env. variables	Coef	R^2	Env. variables	Coef	R^2
High	Pcb	−0.24	0.157			0.103
	Chlorophyll (highly correlated with Pcb)	–		Depth	−0.22	
	Phosphate (negatively correlated with Pcb)	–		Phosphate	−0163	
	Nitrate (negatively correlated with Pcb)	–				
	Salinity	0.23				
				Temperature	0.09	
Low	Temperature	0.045		Pcb	−0.02	
				Chlorophyll (correlated with Pcb)		
				Nitrate (negatively correlated with Pcb)		
No impact	FPI			FPI		
	Depth			Salinity		

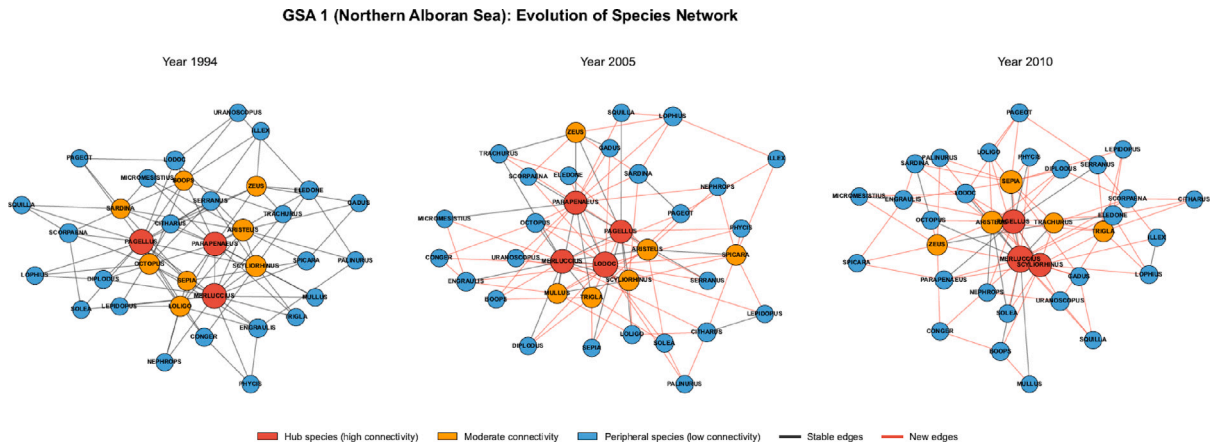

Fig. 8. Spatio-temporal evolution of the species interaction network in GSA 1 (Northern Alboran Sea) for the years 1994, 2005, and 2010. Nodes represent species and edges indicate co-occurrences. To improve readability, edges are displayed with a lower visual weight than nodes, and only the strongest co-occurrence links are shown. Species identified as key nodes for a given year are highlighted using a distinct node encoding, allowing direct visual comparison of changes in key nodes and supporting the Temporal Variation values reported by the framework.

Table 10
Results of the multiple linear regression performed on the temporal diversity of the GSA 7 belonging to the cluster 5. The explanatory variables are sorted according to their influence. The variables having high impact on diversity have a coefficient significantly different from 0.

Impact on diversity	GSA 7		
	Env. variables	Coef	R^2
High	FPI	−0.32	0.23
	Nitrate (highly correlated with FPI)	–	
	Phosphate	0.17	
	Depth	−0.11	
	Salinity (correlated with depth)	–	
Low	Chlorophyll	0.06	
	Pcb (correlated with chlorophyll)	–	
	Temperature (negatively correlated with chlorophyll)	–	

Table 11
Results of the multiple linear regression performed on the temporal diversity of the GSA 2. The explanatory variables are sorted according to their influence. The variables having high impact on diversity have a coefficient significantly different from 0.

Impact on diversity	GSA 2		
	Env. variables	Coef	R2
High	Nitrate	−0.615	0.74
	Chlorophyll	0.34	
	Phosphate (correlated with Nitrate)	–	
	Temperature	0.12	
	Salinity (negatively correlated with Temperature)	–	
	FPI (negatively correlated with Temperature)	–	
No impact	Pcb		
	Depth		

3.2. Case study 2

The network of bat species assemblages was constructed (Figure S6), where nodes represent species and links indicate co-occurrence at the same site. Using species functional distances, we computed temporal diversity and temporal variation, as well as pairwise community dissimilarity ((26) and (28)), as reported in Tables 3 and A.2, respectively.

Table 12
Results of the multiple linear regression performed on the temporal diversity of the GSA 5. The explanatory variables are sorted according to their influence. The variables having high impact on diversity have a coefficient significantly different from 0.

Impact on diversity	GSA 5		
	Env. variables	Coef	R2
High	Depth	0.6	0.78
	Phosphate	0.39	
	Pcb	−0.122	
Low	Chlorophyll (highly correlated with Temperature)	–	
	Nitrate (correlated with Phosphate)	–	
No impact	Temperature		
	FPI		
	Salinity		

Table 13
Results of the multiple linear regression performed on the temporal diversity of the GSA 8. The explanatory variables are sorted according to their influence. The variables having high impact on diversity have a coefficient significantly different from 0.

Impact on diversity	GSA 8		
	Env. variables	Coef	R2
High	FPI	−0.269	0.244
	Depth	−0.165	
	Salinity	0.127	
	Nitrate (negatively correlated with salinity)	–	
Low	Temperature (negatively correlated with salinity)	–	
No impact	Phosphate		
	Pcb		
	Chlorophyll		

The results showed that smaller fragments exhibit lower temporal diversity, with species richness higher in larger and continuous habitats. Temporal variation, on the other hand, was highest in small fragments, revealing significant changes in species co-occurrence and functional distances over time, while larger fragments and continuous forests displayed more stable communities. Pairwise community dissimilarity revealed that bat communities varied over time across all habitats, with these changes being more pronounced in smaller fragments, mainly due

Table 14
Results of the multiple linear regression performed on the temporal diversity of the GSA 10. The explanatory variables are sorted according to their influence. The variables having high impact on diversity have a coefficient significantly different from 0.

Impact on diversity	GSA 10		
	Env. variables	Coef	R2
High	Phosphate	0.27	0.152
	Chlorophyll	−0.25	
	Pcb (highly correlated with Chlorophyll)	–	
	Temperature (negative correlation with phosphate)	–	
Low	Nitrate (highly correlated with phosphate)	–	
	Salinity (negatively correlated with phosphate)	–	
No impact	Depth		
	FPI		

Table 15
Results of the multiple linear regression performed on the temporal diversity of the GSA 15. The explanatory variables are sorted according to their influence. The variables having high impact on diversity have a coefficient significantly different from 0.

Impact on diversity	GSA 15		
	Env. variables	Coef	R2
High	Temperature	−0.64	0.55
	Salinity	−0.35	
	Pcb	−0.16	
	Chlorophyll (highly correlated with Pcb)	–	
	Nitrate (negatively correlated with Temperature)	–	
Low	Phosphate	0.057	
	Depth (correlated with phosphate)	–	
No impact	FPI		

Table 16
Results of the multiple linear regression performed on the temporal diversity of the GSA 20. The explanatory variables are sorted according to their influence. The variables having high impact on diversity have a coefficient significantly different from 0.

Impact on diversity	GSA 20		
	Env. variables	Coef	R2
High	Temperature	−0.65	0.75
	FPI	0.27	

Table 17
Results of the multiple linear regression performed on the temporal diversity of the GSA 22. The explanatory variables are sorted according to their influence. The variables having high impact on diversity have a coefficient significantly different from 0.

Impact on diversity	GSA 22		
	Env. variables	Coef	R2
High	Nitrate	0.5	0.42
	Depth	−0.45	
	Salinity (correlated with Depth)	–	
	FPI (negatively correlated with Depth)	–	
	Temperature (negatively correlated with Depth)	–	
	Phosphate (correlated with Nitrate)	–	
No impact	Pcb		
	Chlorophyll		

Table 18
Results of the multiple linear regression performed on the temporal diversity of the GSA 23. The explanatory variables are sorted according to their influence. The variables having high impact on diversity have a coefficient significantly different from 0.

Impact on diversity	GSA 23		
	Env. variables	Coef	R2
High	Phosphate	0.94	0.83
	Temperature	0.27	
	Chlorophyll	−0.24	
	Pcb (highly correlated with Chlorophyll)	–	
	Nitrate (correlated with Chlorophyll)	–	
	FPI (correlated with Phosphate)	–	
No impact	Depth		
	Salinity		

Table 19
Results of the multiple linear regression performed on the temporal diversity of the GSA 25. The explanatory variables are sorted according to their influence. The variables having high impact on diversity have a coefficient significantly different from 0.

Impact on diversity	GSA 25		
	Env. variables	Coef	R2
High	Salinity	0.4	0.5
	FPI	−0.37	
	Phosphate (negatively correlated with FPI)	–	
	Pcb	0.26	
No impact	Depth		
	Temperature		
	Chlorophyll		
	Nitrate		

to species turnover (Table A.2). In contrast, continuous forests exhibited higher stability in both species turnover and pairwise differences. These findings aligned with the results from temporal variation, confirming that smaller fragments experienced more drastic changes in bat species assemblages. Overall, these results emphasize the importance of protecting large and continuous Amazonian forest habitats from fires and human intervention to maintain stable bat communities.

4. Discussion

It is crucial to understand how communities change over time and space, and how they are influenced by environmental and anthropogenic conditions, in order to obtain a better assessment of ecosystems and to predict their trajectories. Ecological communities can be described and analyzed using diversity measures. Many measures based on Hill numbers offer frameworks for assessing assemblage diversity. Yet, they lack some essential aspects to simultaneously account for species differences (e.g., functional, phylogenetic, or taxonomic distances), the topology of networks, and the time dimension, while these informations are necessary to provide a deeper and more precise understanding of community structure and dynamics. Existing tools for community dynamics and temporal compositional change provide quantitative assessment. For instance, codyn package summarizes changes in community properties through time from species by time matrices, while betapart package quantifies temporal beta diversity and decomposes differences in assemblage composition into turnover and nestedness components (Hallett et al., 2016; Baselga and Orme, 2012). Our framework is not intended to replace these approaches, but to extend temporal analyses by explicitly incorporating network structure and species difference information. By combining time specific co-occurrence networks with inter-specific differences

informed Hill number extensions, it enables the assessment of temporal change not only in species composition or their quantitative component (e.g. abundance, biomass or coverage), but also in the configuration and strength of species associations, thereby offering an additional layer of inference for temporal biodiversity monitoring and conservation planning. It places strong emphasis on using features derived from the graph representation of community diversity, offering several advantages. Firstly, graphical representation provides a robust visual means of illustrating species relationships, simplifying the interpretation of complex biodiversity data. This visualization not only allows researchers to quickly identify patterns, connections, and trends in ecological communities, but also provides an intuitive way to communicate findings to a broader audience, including policymakers and conservationists. Additionally, graph-based models are inherently flexible, as they can integrate multiple types of biodiversity data into a unified framework. For example, they can accommodate species differences or relationships, genetic similarities, habitat associations, and spatial distributions (Dormann et al., 2009). This adaptability enables the integration of diverse sources of information within a unified biodiversity assessment framework. Moreover, this representation excels at simplifying the identification of species and distinct ecological communities, as each connected network can represent a cluster of species. Diversity measures should also take into account the structure of the network, providing insights into the local or global associations of each species with the other species of the assemblage. The proposed framework introduces a new measure, the so-called "strength connectivity". It combines the strength of a species (i.e., the sum of the weights of its immediate connections) with a centrality measure to effectively quantify both the intensity of a species' associations with its neighbors and its structural role within the network. On one hand, the strength of a species determines the degree of its association with its neighbors or its ego-network. On the other hand, the centrality of species (or nodes) reflects their structural power within the network (Ghalmane et al., 2020b, 2019; Termos et al., 2025b,a; Al Tfaily et al., 2026). Yet, the proposed framework is not limited to any specific centrality measure. The choice depends on the type of network and the aims of the study. Centrality can be quantified locally using measures such as degree centrality, which captures the immediate influence of a species within its direct neighborhood, or globally using measures such as Closeness or Betweenness. As a perspective, the framework also has the potential to quantify the hierarchical position of species within the network by using k-core or k-truss centrality. Indeed, k-core (Kong et al., 2019) measures the centrality of a node based on the largest k-core it belongs to, where a k-core is a maximal subgraph in which all nodes have at least k connections within the subgraph. It highlights nodes that are part of densely connected regions (Seidman, 1983). K-truss centrality evaluates a node's centrality by the largest k-truss it belongs to, where a k-truss is a maximal subgraph in which every edge is part of at least (k-2) triangles, emphasizing strongly cohesive substructures (see an application in Ghalmane et al. (2018)). Therefore, the proposed framework uses more information regarding the 'association' between species compared to existing measures, by incorporating their structural power and position within the network, and it remains adaptable through the inclusion of different centrality measures according to the aims of the study. In addition, one critical limitation of many existing biodiversity indices and measures is that they fail to differentiate certain assemblages despite different topological structures, even when species proportions are similar. This limitation often obscures differences in community organization and the underlying ecological processes. By assessing diversity through graph-based measures, the proposed framework avoids such oversights. For example, it becomes possible to differentiate cases where two assemblages have the same diversity but totally different topological structures (see example in Fig. 2). Such distinctions are crucial for conservation planning, where preserving interaction networks may be as important as protecting individual species (Tylianakis et al., 2010).

Biodiversity has a variety of components, whereas most ecological diversity measures summarize only information concerning the relative abundances or richness of species. Nevertheless, in practice, data on species abundance are sometimes unknown. Other measures rely solely on the co-occurrence distance between species without reflecting other types of distances (i.e., taxonomic, phylogenetic, or functional distances). The inclusion of all the different distances between species provides a more detailed quantification and assessment of community diversity. There has been much discussion about the importance of considering the various aspects of diversity for management decisions (Chao and Chiu, 2016; Ohlmann et al., 2019). The framework introduced here enables these informations to be assessed either independently or in combination, allowing for a more meaningful decision to be made. In this case, the network is weighted by the elements of one of the distance matrices. Unweighted networks also constitute a particular case of our framework when only presence/absence data are available. Here, the proposed framework allows these aspects to be measured separately and combined with each other while measuring the strength of species, thereby providing more information on the biodiversity of the ecosystem under study.

Additionally, a third major advantage of the framework is the introduction of two global diversity indices to study the variability of species across time, as well as pairwise community dissimilarity indices. These temporal indices are particularly well-suited for studying dynamic communities, as they allow for the examination of changes across multiple timestamps. This approach can shed light on the resilience and stability of communities under changing environmental conditions, such as habitat disturbance, climate change, invasive species, or other anthropogenic forcings. For instance, temporal analysis may reveal whether key species maintain their central roles over time or whether shifts in network structure signal the onset of instability or collapse (Blonder et al., 2014). Temporal indices can also be used to assess species turnover (i.e., the replacement of one species by another in a community) and association rewiring (the formation of new associations or loss of existing ones). These indices are particularly valuable for understanding how communities respond to external pressures. For example, in a pollination network, the extinction of certain plant species might prompt pollinators to form novel associations with alternative resources, thereby maintaining network functionality despite species loss (Burkle et al., 2013). In conservation biology, temporal network analysis could help predict future biodiversity trends by simulating the effects of specific environmental scenarios. Such predictions are essential for proactive management, allowing stakeholders to intervene before critical thresholds are crossed, leading to irreversible changes in ecosystem structure and function.

In this work, we considered toy examples with known characteristics and differences among species to demonstrate the usefulness and effectiveness of our proposed framework. The consistent results obtained from these toy examples provide preliminary validation of the framework's ability to accurately assess community diversity. We then applied the proposed framework to two real-world datasets with a temporal dimension, previously analyzed using traditional diversity approaches, in order to uncover novel and complementary insights. The temporal resolution of the data available imposed the use of a one-year time window to analyze community diversity dynamics for both the MEDITS and Amazonian datasets (i.e., yearly sampling). While this approach allowed for the generation of comprehensive species networks representative of community complexity, it introduces certain limitations that must be considered when interpreting the results. A one-year time step might mask short-term ecological dynamics, such as seasonal variations in species composition, migration patterns, or reproductive cycles (critical components of biodiversity). For example, many species in both the Mediterranean Sea and Amazonian ecosystems may exhibit seasonal fluctuations driven by environmental changes such as temperature or productivity cycles (M. Milazzo, 2002). Capturing these

finer-scale variations would provide a more nuanced understanding of species associations and their temporal variability.

In addition, annual sampling may oversimplify the underlying processes driving biodiversity changes. For instance, some abrupt events, such as extreme weather, habitat disturbances, or fishing peaks, may influence community structure within a shorter timeframe (Jentsch and Beierkuhnlein, 2008). These events could contribute significantly to biodiversity patterns but remain undetected when using yearly data. The ability to detect rapid responses of communities to sudden environmental changes (e.g., marine heatwaves, deforestation, or pollution) is constrained by yearly sampling. Such responses often involve short-term shifts in species interactions and abundances that could provide valuable insights into ecosystem resilience and vulnerability (Haddad et al., 2015). In addition, while annual data offer a macro-scale view, studies could explore multi-scale temporal approaches by integrating data at both short- and long-term scales when available. For instance, combining multi-annual datasets (as in this study) with finer-scale seasonal or event-driven datasets could reveal interactions between long-term trends and short-term fluctuations (Lindenmayer et al., 2010).

Despite the limitations of a one-year time step, our analyses on both case studies demonstrate the strength of the proposed framework in capturing meaningful temporal trends in community diversity. Regarding fish communities in the Mediterranean Sea, by considering structural properties of species networks and incorporating explanatory variables such as fishing pressure, depth, and temperature, the framework effectively distinguishes between areas with varying biodiversity trends and drivers. For instance, the observed differences in temporal diversity between GSAs 7 and 9 highlight the framework's capacity to detect regional ecological dynamics influenced by environmental variables, even with annual sampling. Similarly, the clustering of GSAs based on shared explanatory variables suggests that the framework provides actionable insights for biodiversity management despite temporal resolution constraints. This is particularly valuable as in the Mediterranean Sea, to date, the most extensive spatial–temporal analysis on demersal fish assemblages, also based on MEDITS data, found no temporal variation in eight traditional diversity indices over two decades (Granger et al., 2015). These indices covered several diversity facets (species number, evenness, and taxonomic, phylogenetic, and functional diversity). All these indices did not highlight temporal differences between communities over time within and among areas (GSAs). Conversely, our new framework, proposing new diversity measures that take into account both distances between species and the structural properties of communities explicitly through time, highlights temporal trends (common in some GSAs, while different in others). In addition to Granger et al. (2015), our work investigated links among diversity patterns with eight explanatory variables (depth, temperature, water salinity, chlorophyll, phosphate, fishing pressure, etc.). Moreover, the GSAs also exhibited different values regarding temporal variation in species. For instance, GSA 1 (Northern Alboran Sea) had the highest value because it had the highest number of species that had undergone major changes over the years in terms of the proportion of strength connectivity compared to other GSAs. Clustering of GSAs based on both temporal indices also provided important insights from a management perspective. Particularly, GSA 7 (Gulf of Lions) is the only GSA that stands alone in a cluster, also knowing that this GSA is the only one having the FPI (Fishing Pressure Index) as the strongest explanatory variable. This GSA had indeed been heavily exploited by professional trawling fisheries before and during the years under study. This also explains why it has the lowest temporal diversity compared to the other GSAs belonging to other clusters. Such results could provide guidance for management perspectives, such as fishing regulations.

We also applied the framework to the Amazonian bats dataset to demonstrate its applicability to different community types, extending beyond marine ecosystems and on a smaller temporal scale (four years of sampling). This highlights the versatility of the framework in capturing temporal diversity trends across ecosystems with varying ecological structures and time frames. It also enables us to evaluate how forest fragmentation can influence the biodiversity of bat assemblages. Forest fragmentation is one of the most pressing drivers of biodiversity loss in tropical landscapes, and its impact on bat assemblages offers valuable insights into the ecological consequences of habitat disruption. In a previous work based on this dataset, Farneda et al. (2015) identified functional traits of bat species such as mobility, body mass, wing morphology, and trophic level as critical determinants of species' vulnerability to fragmentation. Our framework complements and deepens these findings by highlighting that bat species richness and temporal diversity decrease with decreasing fragment size. In addition, our results reveal that small forest fragments exhibit higher temporal variation in species composition compared to larger fragments and continuous forest areas. This variation is primarily driven by species turnover, indicating that fragmented habitats experience shifts in community composition. Such findings align with previous studies showing that fragmented landscapes often experience disrupted ecological dynamics due to edge effects, reduced habitat connectivity, and altered resource availability (Laurance and Bierregaard, 1997; Gorresen et al., 2005). These factors likely exacerbate species turnover by increasing the vulnerability of certain species while favoring others, particularly generalists or edge-adapted species. Habitat fragmentation resulting from fire or human activities decreased bat temporal diversity. Moreover, the lowest diversity was observed more distinctly in small fragments. This suggests that fragmentation not only reduces species richness but also disrupts the stability of ecological communities over time. This is consistent with research showing that temporal stability of diversity decreases under habitat fragmentation, as ecological processes are disrupted (Didham, 1998; Ngila et al., 2024). Overall, these findings reinforce the link between habitat integrity and biodiversity maintenance. The implications of these findings are important for conservation efforts. Habitat fragmentation caused by fire or human activities leads to a measurable decline in bat temporal diversity, with the most pronounced effects observed in small fragments. This underscores the urgency of restoring fragmented landscapes to preserve the biodiversity and ecological functions of bat species in the Amazon rainforest. Conservation strategies should prioritize increasing habitat connectivity, reducing edge effects, and implementing reforestation programs to mitigate the impacts of fragmentation (Haddad et al., 2015). Additionally, the observed patterns in our study suggest that large, continuous forest areas are critical for maintaining both species richness and temporal stability in bat assemblages. Given that bats play key roles as pollinators, seed dispersers, and insect regulators in tropical ecosystems, preserving their diversity is essential for maintaining ecosystem health and resilience. The application of our framework to the Amazonian bats dataset demonstrates its ability to provide novel insights into the temporal dynamics of biodiversity under habitat fragmentation. The findings emphasize the importance of integrating structural and temporal diversity measures into conservation planning to safeguard species diversity in fragmented tropical ecosystems.

Overall, through the analysis of these two case studies, we demonstrate that the proposed framework is not limited to a specific ecological system or data type. Instead, it is a flexible and generalizable approach that can be applied across a wide range of datasets regardless of their temporal extent, spatial resolution, or taxonomic scope. Its adaptability makes it a valuable tool for investigating biodiversity dynamics in aquatic, marine, and terrestrial ecosystems, and for gaining insights into community responses to global, regional, or local changes.

Based on the proposed framework, several perspectives for advancing biodiversity assessment could be investigated. First, when data are available, biodiversity can be assessed more comprehensively by constructing multilayer networks that represent ecological interactions across multiple dimensions, such as trophic (feeding), functional (roles within an ecosystem), and genetic (shared evolutionary traits) layers. In a multilayer network, each layer represents a distinct type

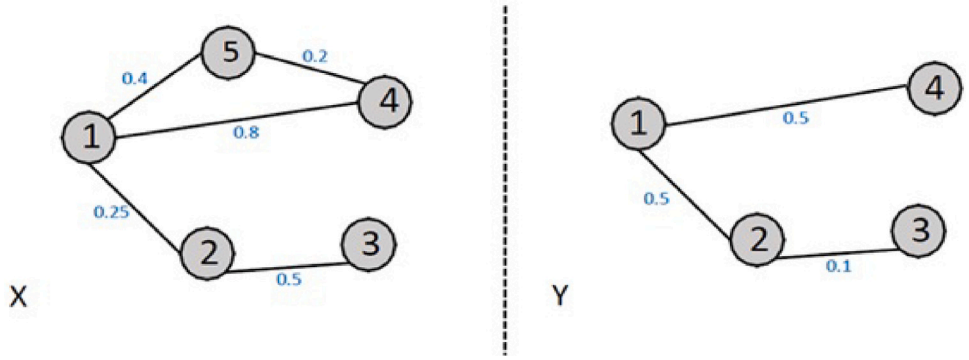

Fig. A.1. A toy example representing the assemblages (networks) X and Y of two pools of species labeled from 1 to 5. The links between species represent species co-occurence based on species presence-absence data, or quantitative data (e.g., species abundance, biomass, or coverage). In the case of the availability of the pairwise distances between species, such as functional, phylogenetic or taxonomic ones, values in blue are the extent of these distances.

Table A.1
The values of the Strength connectivity (SC) of species belonging to both assemblages.

Community	Shared species						All the species					
	X			Y			X			Y		
Measure	Degree	Strength	SC	Degree	Strength	SC	Degree	Strength	SC	Degree	Strength	SC
Species 1	1	1	1,41	1	1	1,41	1	1	1,41	1	1	1,41
Species 2	1	0,6	1,17	1	0,71	1,23	0,66	0,52	0,84	1	0,71	1,23
Species 3	0,5	0,1	0,51	0,5	0,47	0,69	0,33	0,34	0,47	0,5	0,47	0,69
Species 4	0,5	0,5	0,71	0,5	0,76	0,91	0,66	0,69	0,95	0,5	0,76	0,91
Species 5	–	–	–	–	–	–	0,66	0,41	0,78	–	–	–

X and Y in the toy example of Fig. A.1. It is computed based on species pairwise distances (e.g., functional, phylogenetic or taxonomic distances between species).

Table A.2
The pairwise differences computed for each type of habitat between every two consecutive years.

Habitat	Measure	2011–2012	2012–2013	2013–2014	Average	Standard deviation
1 ha fragments	β_{ST}	0,51	0,62	0,46	0,53	0,08
	β_{OS}	0,31	0,16	0,38	0,28	0,11
	β_{WN}	0,82	0,78	0,84	0,81	0,03
10 ha fragments	β_{ST}	0,53	0,5	0,59	0,54	0,05
	β_{OS}	0,17	0,22	0,11	0,17	0,06
	β_{WN}	0,7	0,72	0,7	0,71	0,01
100 ha fragments	β_{ST}	0,34	0,32	0,33	0,33	0,01
	β_{OS}	0,21	0,32	0,17	0,23	0,08
	β_{WN}	0,55	0,64	0,5	0,56	0,07
Continuous forest	β_{ST}	0,11	0,14	0,14	0,13	0,02
	β_{OS}	0,3	0,25	0,26	0,27	0,03
	β_{WN}	0,41	0,39	0,4	0,40	0,01

of interaction, while interlayer connections capture how species or nodes contribute across these dimensions. This approach provides a holistic view of community structure and function by accounting for the multidimensionality of ecosystems (Pilosof et al., 2017). For instance, a multilayer network could simultaneously capture pollination, predation, and competition interactions, allowing researchers to assess the interplay between these processes and their contributions to ecosystem stability (Kéfi et al., 2016). Furthermore, multilayer networks help identify species that act as keystone connectors across multiple layers, such as generalist pollinators that maintain both pollination and seed-dispersal functions. By focusing on interdependencies across layers, this perspective enables the detection of vulnerabilities in ecosystems that might not be apparent when examining only a single interaction type. The integration of multilayer networks into biodiversity studies also offers practical applications for conservation planning. For example, habitat restoration efforts could prioritize species that maintain connectivity across layers, thereby safeguarding multiple ecosystem functions simultaneously (Miele et al., 2019). These insights underscore the potential of multilayer networks (particularly when combined with the temporal dimension and the proposed framework) to enhance our understanding of ecosystem complexity and the cascading effects of environmental disturbances.

The proposed framework can also contribute significantly to the understanding and management of ecosystem functions and services; the benefits that humans derive from ecosystems, such as pollination, water purification, and carbon sequestration. By linking network structure to ecosystem functions, it becomes possible to assess how changes in biodiversity over time impact the stability and productivity of ecosystems (Isbell et al., 2011). For instance, species with high centrality or strength connectivity in ecological networks often play disproportionate roles in maintaining ecosystem functions. In a pollination network, these might include generalist pollinators that connect multiple plant species, ensuring stable crop production and biodiversity. Identifying and prioritizing the conservation of such species

through the framework can enhance ecosystem resilience in the face of environmental change (Garibaldi et al., 2013). Furthermore, this approach allows for a spatially explicit understanding of ecosystem services, as network analysis can reveal how the spatial arrangement of habitats affects species interactions and functional outcomes. For example, fragmented habitats often exhibit reduced connectivity in species networks, impairing critical services such as seed dispersal (Kremen and Merenlender, 2018). By applying network-based biodiversity measures, the framework provides actionable insights for management and ecological restoration. Finally, it is important to emphasize that the proposed framework is generalizable and can be applied to any ecological dataset containing temporal information on species composition, whether based on abundance, biomass, presence-absence data, or other quantitative measures. This flexibility stems from the framework's modular design, which allows researchers to incorporate various types of species differences (functional, phylogenetic, taxonomic) according to data availability, while the core temporal diversity and variation measures remain applicable regardless of the specific ecological system, taxonomic group, or spatial scale under study.

Furthermore, the most computationally demanding steps of the proposed framework are the construction of co-occurrence networks and the calculation of strength connectivity, which are performed separately for each time unit using the data available for that unit. These steps rely on species occurrence or quantitative data (e.g. abundance, biomass or coverage) and on fixed species difference matrices that are reused across time units, and therefore do not require information from other temporal slices at this stage (Poisot et al., 2015). As a consequence, network construction and strength connectivity calculations can be executed independently across time units and are well suited to parallel execution on multi core machines, high performance computing clusters, or cloud based infrastructures (Newman, 2018). Subsequent steps required to compute the temporal indices involve aggregating results across time units, which introduces logical dependencies but remains computationally lightweight compared to network construction (Newman, 2018). Overall computational demand increases with the number of species, samples, and temporal resolution, a pattern that is widely recognized in ecological network analyses and their methodological constraints (Dormann et al., 2017). For large datasets or high frequency monitoring programs, distributing computations across time units or spatial subsets substantially reduces runtime without altering the conceptual structure of the analyses (Newman, 2018). Additional scalability can be achieved through temporal aggregation or justified filtering of rare species, provided that these choices are aligned with the ecological questions addressed and with known limitations of co-occurrence based inference (Blanchet et al., 2020; Dormann et al., 2017). Consequently, the framework is not limited by data volume per se, but by the availability of appropriate computational resources and transparent reporting of analytical settings, which is consistent with best practices in community dynamics and related toolkit.

5. Conclusion

This paper provides a methodological framework to assess temporal change in community diversity by integrating species differences, network structure, and time. The approach quantifies how communities evolve through two complementary indices, temporal diversity and temporal variation, both computed from strength connectivity within time specific networks. When required, an optional module also provides pairwise community dissimilarity across time units to support direct time to time comparisons. The proposed framework can be applied to any faunal/floristic terrestrial or aquatic/marine communities. It is a generalizable approach to assess and understand ecological and anthropogenic phenomena that may apply across the tree of life. Interestingly, this framework allows quantification of the diversity of species based on their strength connectivity instead of their proportion (e.g., abundance, biomass, etc.) or probability of association. This measure accounts for the structure of the network to eliminate cases where assemblages have the same diversity while having different structures. The second strong point of this framework is its incorporation of all the various distances between species (i.e., functional, phylogenetic or taxonomic distances). Additionally, the proposed framework also introduces two overall measures and pairwise community dissimilarity measures. By applying the new framework to two distinct datasets, we showed its capacity to capture complementary and previously overlooked patterns, enabling a deeper understanding of community dynamics and their responses to environmental and anthropogenic changes. We thus believe that the proposed framework should now pave the way for a better assessment of the spatial and temporal biodiversity, and contribute to its management and conservation. Further improvements of the framework to achieve deeper biodiversity assessments are possible. As a follow-up to this work, more sophisticated centrality measures could be considered to tailor various types of structures. This will involve incorporating a broader range of micro- and macro-information on the species networks to enhance the accuracy and comprehensiveness of the variation in diversity. The integration of these perspectives into the proposed framework emphasizes its potential to address pressing ecological challenges. Notably, by adopting multilayer networks and ecosystem service analyses, researchers can gain a deeper understanding of how biodiversity, ecosystem functions and services interact across spatial, temporal, and functional dimensions. Such a framework should not only advance theoretical ecology but also offer practical solutions for managing biodiversity in a rapidly changing world.

CRediT authorship contribution statement

Zakariya Ghalmane: Writing – review & editing, Writing – original draft, Visualization, Validation, Software, Methodology, Investigation, Formal analysis, Conceptualization. **Pascal Poncelet:** Review & editing, Validation, Supervision. **Roberto Interdonado:** Review & editing, Validation, Supervision. **Dino Ienco:** Review & editing, Validation, Supervision. **Pierluigi Carbonara:** Data curation. **Angelo Cau:** Data curation. **Antonio Esteban:** Data curation. **Maria Teresa Farriols:** Review & editing, Data curation. **Maria Cristina Follesa:** Data curation. **Cristina Garcia-Ruiz:** Data curation. **Germana Garofalo:** Data curation. **Gioacchino Bono:** Data curation. **Taha Imzilen:** Data curation. **Igor Isajlović:** Data curation. **Stefanos Kavadas:** Data curation. **Irida Maina:** Data curation. **Porzia Maiorano:** Review & editing, Data curation. **Chiara Manfredi:** Data curation. **Jurgen Mifsud:** Review & editing, Data curation. **Panagiota Peristeraki:** Data curation. **Mario Sbrana:** Data curation. **Maria Teresa Spedicato:** Data curation. **Ioannis Thasitis:** Review & editing, Data curation. **Nedo Vrgoc:** Data curation. **Bastien Mérigot:** Writing – review & editing, Writing – original draft, Validation, Supervision, Project administration, Methodology, Formal analysis, Conceptualization.

Declaration of competing interest

The authors declare that they have no known competing financial interests or personal relationships that could have appeared to influence the work reported in this paper.

Acknowledgments

We thank three anonymous reviewers for their constructive comments on earlier versions of the manuscript. We are grateful to Michael Paul for correcting the English of the manuscript. This work is the object of the project NETwork modeling for the bioDIVersity of species communities (NETDIV). The research received funding from the LabEx NUMEV laboratory of the University of Montpellier (UM). Z.G. has been funded by UM. B.M. acknowledges funding support from the European

Union's Horizon 2020 research and innovation program under grant agreement no. 101059823 (B-USEFUL). We thank the many people who have been involved in collecting biological data in the frame of the MEDITS survey that was performed under the Data Collection Framework (DFC) and in organizing surveys at sea.

Appendix A. My appendix

The Fig. A.1 and Tables A.1–A.2 provided in the appendix offer to detail a toy example using species pairwise distances (Fig. A.1 and Table A.1), as well as to provide pairwise community dissimilarity measures computed on the bats dataset (Table A.2).

Appendix B. Supplementary data

Supplementary material related to this article can be found online at https://doi.org/10.1016/j.ecoinf.2026.103716.

Data availability

The code of the proposed framework is available online at https://github.com/zakariyaGH/METITS_and_bats_Studies and can be used to compute the three diversity indices introduced in this manuscript. To facilitate reproducibility, we provide the operating environment and minimal instructions used to generate the results. All analyses were performed in Python on a 64-bit system using the NetworkX library for network construction, manipulation, and visualization. The repository contains a script that reproduces the main figures based on the example datasets. After downloading the repository, users can run the main script to rebuild the networks for each time unit and compute temporal diversity, temporal variation, and the optional pairwise community dissimilarity.
The data was collected by the MEDITS program "Mediterranean international trawl survey": https://doi.org/10.3989/scimar.2019.83S1. Data are available on the EU Joint Research Center (JRC): https://data.jrc.ec.europa.eu/dataset/f25092c4-3f0f-449f-ba60-5fbfe385defc.
The Bats data was extracted from the CESTES database, which is a global database for metacommunity ecology, integrating species, traits, environment and space. The data can be found in https://idata.idiv.de/ddm/Data/ShowData/286.

References

Al Tfaily, F., Ghalmane, Z., Brahmia, M.e.A., Hazimeh, H., Jaber, A., Zghal, M., 2025. Graph-based federated learning approach for intrusion detection in IoT networks. Sci. Rep. 15 (1), 41264.
Al Tfaily, F., Ghalmane, Z., Brahmia, M.E.A., Hazimeh, H., Jaber, A., Zghal, M., 2026. Community-based vulnerability prediction framework for iot intrusion detection using only network topology. Future Gener. Comput. Syst. 108493.
Baselga, A., Orme, C.D.L., 2012. Betapart: an R package for the study of beta diversity. Methods Ecol. Evol. 3 (5), 808–812.
Bertrand, J.A., de Sola, L.G., Papaconstantinou, C., Relini, G., Souplet, A., 2002. The general specifications of the MEDITS surveys. Sci. Mar. 66 (S2), 9–17.
Blanchet, F.G., Cazelles, K., Gravel, D., 2020. Co-occurrence is not evidence of ecological interactions. Ecol. Lett. 23 (7), 1050–1063.
Blonder, B., Lamanna, C., Violle, C., Enquist, B.J., 2014. The n-dimensional hypervolume. Glob. Ecol. Biogeogr. 23 (5), 595–609.
Burkle, L.A., Marlin, J.C., Knight, T.M., 2013. Plant-pollinator interactions over 120 years: loss of species, co-occurrence, and function. Science 339 (6127), 1611–1615.
CaraDonna, P.J., Petry, W.K., Brennan, R.M., Cunningham, J.L., Bronstein, J.L., Waser, N.M., Sanders, N.J., 2017. Interaction rewiring and the rapid turnover of plant–pollinator networks. Ecol. Lett. 20 (3), 385–394.
Chao, A., Chiu, C.-H., 2016. Bridging the variance and diversity decomposition approaches to beta diversity via similarity and differentiation measures. Methods Ecol. Evol. 7 (8), 919–928.
Chao, A., Chiu, C.-H., Jost, L., 2010. Phylogenetic diversity measures based on Hill numbers. Phil. Trans. R. Soc. B 365 (1558), 3599–3609.
Chao, A., Gotelli, N.J., Hsieh, T., Sander, E.L., Ma, K., Colwell, R.K., Ellison, A.M., 2014. Rarefaction and extrapolation with Hill numbers: a framework for sampling and estimation in species diversity studies. Ecol. Monograph. 84 (1), 45–67.
Coll, M., Piroddi, C., Albouy, C., Ben Rais Lasram, F., Cheung, W.W., Christensen, V., Karpouzi, V.S., Guilhaumon, F., Mouillot, D., Paleczny, M., et al., 2012. The Mediterranean Sea under siege: spatial overlap between marine biodiversity, cumulative threats and marine reserves. Glob. Ecol. Biogeogr. 21 (4), 465–480.
Coll, M., Piroddi, C., Steenbeek, J., Kaschner, K., Ben Rais Lasram, F., Aguzzi, J., Ballesteros, E., Bianchi, C.N., Corbera, J., Dailianis, T., et al., 2010. The biodiversity of the Mediterranean Sea: estimates, patterns, and threats. PloS One 5 (8), e11842.
Das, K., Samanta, S., Pal, M., 2018. Study on centrality measures in social networks: a survey. Soc. Netw. Anal. Min. 8 (1), 1–11.
Delmas, E., Besson, M., Brice, M.-H., Burkle, L.A., Dalla Riva, G.V., Fortin, M.-J., Gravel, D., Guimarães, Jr., P.R., Hembry, D.H., Newman, E.A., et al., 2019. Analysing ecological networks of species interactions. Biol. Rev. 94 (1), 16–36.
Devictor, V., Mouillot, D., Meynard, C., Jiguet, F., Thuiller, W., Mouquet, N., 2010. Spatial mismatch and congruence between taxonomic, phylogenetic and functional diversity: the need for integrative conservation strategies in a changing world. Ecol. Lett. 13 (8), 1030–1040.
Didham, R.K., 1998. Altered leaf-litter decomposition rates in tropical forest fragments. Oecologia 116 (3), 397–406.
Dormann, C.F., Fründ, J., Blüthgen, N., Gruber, B., 2009. Indices, graphs and null models: analyzing bipartite ecological networks.
Dormann, C.F., Fründ, J., Schaefer, H.M., 2017. Identifying causes of patterns in ecological networks: opportunities and limitations. Annu. Rev. Ecol. Evol. Syst. 48, 559–584.
Farneda, F.Z., Rocha, R., López-Baucells, A., Groenenberg, M., Silva, I., Palmeirim, J.M., Bobrowiec, P.E., Meyer, C.F., 2015. Trait-related responses to habitat fragmentation in Amazonian bats. J. Appl. Ecol. 52 (5), 1381–1391.
Garibaldi, L.A., Steffan-Dewenter, I., Winfree, R., Aizen, M.A., Bommarco, R., Cunningham, S.A., Kremen, C., Carvalheiro, L.G., Harder, L.D., Afik, O., et al., 2013. Wild pollinators enhance fruit set of crops regardless of honey bee abundance. Science 339 (6127), 1608–1611.
Ghalmane, Z., Brahmia, M.-E.-A., Zghal, M., Cherifi, H., 2022. A stochastic approach for extracting community-based backbones. In: International Conference on Complex Networks and their Applications. Springer, pp. 55–67.
Ghalmane, Z., Cherifi, C., Cherifi, H., El Hassouni, M., 2020a. A community-aware backbone extractor for weighted networks. In: 9th International Conference on Complex Networks and their Applications. pp. p–3.
Ghalmane, Z., Cherifi, C., Cherifi, H., El Hassouni, M., 2021. Author correction: Extracting backbones in weighted modular complex networks. Sci. Rep. 11, 8957.
Ghalmane, Z., El Hassouni, M., Cherifi, C., Cherifi, H., 2018. K-truss decomposition for modular centrality. In: 2018 9th International Symposium on Signal, Image, Video and Communications. ISIVC, IEEE, pp. 241–248.
Ghalmane, Z., El Hassouni, M., Cherifi, C., Cherifi, H., 2019. Centrality in modular networks. EPJ Data Sci. 8 (1), 1–27.
Ghalmane, Z., Rajeh, S., Cherifi, C., Cherifi, H., El Hassouni, M., 2020b. Finding influential nodes in networks with community structure. In: Network Modeling, Learning and Analysis (NMLA), WorldCIST2020 Workshop. p. 3.
Gorresen, P.M., Willig, M.R., Strauss, R.E., 2005. Multivariate analysis of scale-dependent associations between bats and landscape structure. Ecol. Appl. 15 (6), 2126–2136.
Granger, V., Fromentin, J.-M., Bez, N., Relini, G., Meynard, C.N., Gaertner, J.-C., Maiorano, P., Ruiz, C.G., Follesa, C., Gristina, M., et al., 2015. Large-scale spatio-temporal monitoring highlights hotspots of demersal fish diversity in the Mediterranean Sea. Prog. Oceanogr. 130, 65–74.
Haddad, N.M., Brudvig, L.A., Clobert, J., Davies, K.F., Gonzalez, A., Holt, R.D., Lovejoy, T.E., Sexton, J.O., Austin, M.P., Collins, C.D., et al., 2015. Habitat fragmentation and its lasting impact on Earth's ecosystems. Sci. Adv. 1 (2), e1500052.
Hallett, L.M., Jones, S.K., MacDonald, A.A.M., Jones, M.B., Flynn, D.F., Ripplinger, J., Slaughter, P., Gries, C., Collins, S.L., 2016. Codyn: An r package of community dynamics metrics. Methods Ecol. Evol. 7 (10), 1146–1151.
Hill, M.O., 1973. Diversity and evenness: a unifying notation and its consequences. Ecology 54 (2), 427–432.
Interdonato, R., Tagarelli, A., Ienco, D., Sallaberry, A., Poncelet, P., 2017. Local community detection in multilayer networks. Data Min. Knowl. Discov. 31 (5), 1444–1479.
Isbell, F., Calcagno, V., Hector, A., Connolly, J., Harpole, W.S., Reich, P.B., Scherer-Lorenzen, M., Schmid, B., Tilman, D., Van Ruijven, J., et al., 2011. High plant diversity is needed to maintain ecosystem services. Nature 477 (7363), 199–202.
Jacoby, D.M., Freeman, R., 2016. Emerging network-based tools in movement ecology. Trends Ecol. Evolut. 31 (4), 301–314.
Jentsch, A., Beierkuhnlein, C., 2008. Research frontiers in climate change: effects of extreme meteorological events on ecosystems. C. R. Geosci. 340 (9–10), 621–628.
Jost, L., 2006. Entropy and diversity. Oikos 113 (2), 363–375.
Jost, L., 2007. Partitioning diversity into independent alpha and beta components. Ecology 88 (10), 2427–2439.
Kéfi, S., Miele, V., Wieters, E.A., Navarrete, S.A., Berlow, E.L., 2016. How structured is the entangled bank? The surprisingly simple organization of multiplex ecological networks leads to increased persistence and resilience. PLoS Biol. 14 (8), e1002527.
Koleff, P., Gaston, K.J., Lennon, J.J., 2003. Measuring beta diversity for presence–absence data. J. Anim. Ecol. 72 (3), 367–382.

Kong, Y.-X., Shi, G.-Y., Wu, R.-J., Zhang, Y.-C., 2019. K-core: Theories and applications. Phys. Rep. 832, 1–32.
Kremen, C., Merenlender, A.M., 2018. Landscapes that work for biodiversity and people. Science 362 (6412), eaau6020.
Lasram, F.B.R., Guilhaumon, F., Mouillot, D., 2009. Fish diversity patterns in the Mediterranean Sea: deviations from a mid-domain model. Mar. Ecol. Prog. Ser. 376, 253–267.
Laurance, W.F., Bierregaard, R.O., 1997. Tropical Forest Remnants: Ecology, Management, and Conservation of Fragmented Communities. University of Chicago Press.
Lefcheck, J.S., Buchheister, A., Laumann, K.M., Stratton, M.A., Sobocinski, K.L., Chak, S.T., Clardy, T.R., Reynolds, P.L., Latour, R.J., Duffy, J.E., 2014. Dimensions of biodiversity in Chesapeake Bay demersal fishes: patterns and drivers through space and time. Ecosphere 5 (2), 1–48.
Legras, G., Loiseau, N., Gaertner, J.-C., Poggiale, J.-C., Ienco, D., Mazouni, N., Mérigot, B., 2019a. Assessment of congruence between co-occurrence and functional networks: A new framework for revealing community assembly rules. Sci. Rep. 9 (1), 1–10.
Legras, G., Loiseau, N., Gaertner, J.-C., Poggiale, J.-C., Ienco, D., Mazouni, N., Mérigot, B., 2019b. Assessment of congruence between co-occurrence and functional networks: A new framework for revealing community assembly rules. Sci. Rep. 9 (1), 1–10.
Lindenmayer, D.B., Likens, G., Krebs, C., Hobbs, R., 2010. Improved probability of detection of ecological "surprises". Proc. Natl. Acad. Sci. 107 (51), 21957–21962.
Loiseau, N., Legras, G., Gaertner, J.-C., Verley, P., Chabanet, P., Mérigot, B., 2017. Performance of partitioning functional beta-diversity indices: Influence of functional representation and partitioning methods. Glob. Ecol. Biogeogr. 26 (6), 753–762.
M. Milazzo, e.a., 2002. Daily and seasonal variability in the assemblage structure of fish in shallow Mediterranean rocky reefs. J. Mar. Biol. Assoc. UK 82 (5), 853–862.
Magurran, A.E., 2013. Measuring Biological Diversity. John Wiley & Sons.
Magurran, A.E., McGill, B.J., 2011. Biological Diversity: Frontiers in Measurement and Assessment. Oxford University Press.
Martínez-López, J., Bertzky, B., Robuchon, M., Bonet, F.J., Dubois, G., 2023. Assessing habitat diversity and potential areas of similarity across protected areas globally. Ecol. Inform. 75, 102090.
Mérigot, B., Gaertner, J.-C., Brind'Amour, A., Carbonara, P., Esteban, A., Garcia-Ruiz, C., Gristina, M., Imzilen, T., Jadaud, A., Joksimovic, A., et al., 2019. Stability of the relationships among demersal fish assemblages and environmental-trawling drivers at large spatio-temporal scales in the northern Mediterranean Sea. Sci. Mar. 83 (S1), 153–163.
Miele, V., Railsback, S.F., Kéfi, S., 2019. Eco-evolutionary dynamics of nested and modular multilayer ecological networks. Ecol. Lett. 22 (1), 71–80.
Mouillot, D., Albouy, C., Guilhaumon, F., Lasram, F.B.R., Coll, M., Devictor, V., Meynard, C.N., Pauly, D., Tomasini, J.A., Troussellier, M., et al., 2011. Protected and threatened components of fish biodiversity in the Mediterranean Sea. Curr. Biol. 21 (12), 1044–1050.
Newman, M., 2018. Networks. Oxford University Press.
Ngila, P.M., Danmallam, B.A., Iniunam, I.A., Kuria, A., Trevelyan, R., 2024. Impact of forest cover loss on forest dependent avian species in Kenya. Sci. Afr. 26, e02463.
Ohlmann, M., Miele, V., Dray, S., Chalmandrier, L., O'connor, L., Thuiller, W., 2019. Diversity indices for ecological networks: a unifying framework using hill numbers. Ecol. Lett. 22 (4), 737–747.
Opsahl, T., Agneessens, F., Skvoretz, J., 2010. Node centrality in weighted networks: Generalizing degree and shortest paths. Soc. Netw. 32 (3), 245–251.
Pavoine, S., 2012. Clarifying and developing analyses of biodiversity: towards a generalisation of current approaches. Methods Ecol. Evol. 3 (3), 509–518.
Peet, R.K., 1974. The measurement of species diversity. Annu. Rev. Ecol. Syst. 5 (1), 285–307.
Pilosof, S., Porter, M.A., Pascual, M., Kéfi, S., 2017. The multilayer nature of ecological networks. Nat. Ecol. Evol. 1 (4), 0101.
Poisot, T., 2022. Dissimilarity of species interaction networks: quantifying the effect of turnover and rewiring. Peer Community J. 2.
Poisot, T., Canard, E., Mouillot, D., Mouquet, N., Gravel, D., 2012. The dissimilarity of species interaction networks. Ecol. Lett. 15 (12), 1353–1361.
Poisot, T., Stouffer, D.B., Gravel, D., 2015. Beyond species: why ecological interaction networks vary through space and time. Oikos 124 (3), 243–251.
Rao, C.R., 1982. Diversity and dissimilarity coefficients: a unified approach. Theor. Popul. Biol. 21 (1), 24–43.
Salathé, M., Jones, J.H., 2010. Dynamics and control of diseases in networks with community structure. PLoS Comput. Biol. 6 (4), e1000736.
Scheiner, S.M., 2012. A metric of biodiversity that integrates abundance, phylogeny, and function. Oikos 121 (8), 1191–1202.
Seidman, S.B., 1983. Network structure and minimum degree. Soc. Netw. 5 (3), 269–287.
Siwicka, E., Thrush, S.F., Hewitt, J.E., 2020. Linking changes in species–trait relationships and ecosystem function using a network analysis of traits. Ecol. Appl. 30 (1), e02010.
Smith, B., Wilson, J.B., 1996. A consumer's guide to evenness indices. Oikos 70–82.
Socolar, J.B., Gilroy, J.J., Kunin, W.E., Edwards, D.P., 2016. How should beta-diversity inform biodiversity conservation? Trends Ecol. Evolut. 31 (1), 67–80.
Spedicato, M.T., Massutí, E., Mérigot, B., Tserpes, G., Jadaud, A., Relini, G., 2019. The MEDITS trawl survey specifications in an ecosystem approach to fishery management. Sci. Mar. 83 (S1), 9–20.
Stuart-Smith, R.D., Bates, A.E., Lefcheck, J.S., Duffy, J.E., Baker, S.C., Thomson, R.J., Stuart-Smith, J.F., Hill, N.A., Kininmonth, S.J., Airoldi, L., et al., 2013. Integrating abundance and functional traits reveals new global hotspots of fish diversity. Nature 501 (7468), 539–542.
Sutherland, W.J., Freckleton, R.P., Godfray, H.C.J., Beissinger, S.R., Benton, T., Cameron, D.D., Carmel, Y., Coomes, D.A., Coulson, T., Emmerson, M.C., et al., 2013. Identification of 100 fundamental ecological questions. J. Ecol. 101 (1), 58–67.
Termos, M., Ghalmane, Z., Fadlallah, A., Jaber, A., Zghal, M., et al., 2023. Intrusion detection system for iot based on complex networks and machine learning. In: 2023 IEEE Intl Conf on Dependable, Autonomic and Secure Computing, Intl Conf on Pervasive Intelligence and Computing, Intl Conf on Cloud and Big Data Computing, Intl Conf on Cyber Science and Technology Congress (DASC/PiCom/CBDCom/CyberSciTech). IEEE, pp. 0471–0477.
Termos, M., Ghalmane, Z., Fadlallah, A., Jaber, A., Zghal, M., et al., 2025a. Enhancing iot network intrusion detection with a new graphsage embedding algorithm using centrality measures. In: 10th International Conference on Internet of Things, Big Data and Security. SCITEPRESS-Science and Technology Publications, pp. 329–336.
Termos, M., Ghalmane, Z., Fadlallah, A., Jaber, A., Zghal, M., et al., 2025b. Integrating centrality measures in federated learning-based intrusion detection systems. In: 2025 IEEE Wireless Communications and Networking Conference. WCNC, IEEE, pp. 1–6.
Tylianakis, J.M., Laliberté, E., Nielsen, A., Bascompte, J., 2010. Conservation of species interaction networks. Biol. Cons. 143 (10), 2270–2279.
Tylianakis, J.M., Morris, R.J., 2017. Ecological networks across environmental gradients. Annu. Rev. Ecol. Evol. Syst. 48, 25–48.
Vellend, M., Cornwell, W.K., Magnuson-Ford, K., Mooers, A.Ø., 2011. Measuring phylogenetic biodiversity. In: Biological Diversity: Frontiers in Measurement and Assessment. Oxford University Press, Oxford, pp. 194–207.
Villéger, S., Mason, N.W., Mouillot, D., 2008. New multidimensional functional diversity indices for a multifaceted framework in functional ecology. Ecology 89 (8), 2290–2301.
Violle, C., Navas, M.-L., Vile, D., Kazakou, E., Fortunel, C., Hummel, I., Garnier, E., 2007. Let the concept of trait be functional!. Oikos 116 (5), 882–892.
Weiher, E., 2011. A primer of trait and functional diversity. In: Magurran, A., McGill, B. (Eds.), Biological Diversity: Frontiers in Measurement and Assessment. Oxford University Press, Oxford.